SONNE or METEOR or MARIA S.MERIAN or ALKOR or ELISABETH MANN BORGESE or HEINCKE-Berichte

Reconstructing volcanic eruptions and tsunamis of Krakatau Volcano - Transit

Cruise No. SO299/2

15.08.2023 – 02.09.2023,

Singapore (Singapore) – Port Louis (Mauritius)

REE_T

Morelia Urlaub, Julie Belo, Christian Berndt, Elisa Klein, Jochen Wollschläger, Ann-Marie Völsch

Morelia Urlaub

GEOMAR Helmholtz Centre for Ocean Research Kiel

2023

Table of Contents

1 Cruise Summary

1.1 Summary in English

Cruise SO299/2 of the German Research Vessel SONNE was a transit cruise with four working days. The main scientific focus was on Krakatau archipelago in the Sunda Strait, source of at least two major tsunamis in historic times. Reflection seismic profiles, hydroacoustic data, and sediment cores were collected west, south, and east of the archipelago. Furthermore, bio-optical observations for an improved underwater light field characterization and parametrization within the Indian Ocean were conducted on a transect from Singapore to Mauritius.

The aim of the Krakatau survey was to shed light on the erupted volumes of the disastrous 1883 eruption and to decipher the processes leading to a damaging tsunami. Seismic imaging reveals three seismically different types of deposits, possibly originating from the 1883 events given their proximity to the modern seafloor. They vary in thickness reaching up to 100 m in places. One of the deposits is topped by large blocks with diameters up to 400 m that stick out up to 30 m from the surrounding seafloor. The size and density of blocks decreases with increasing distance to the volcano, which may suggest a debris flow deposit rather than a pyroclastic flow. Normal faults spread around the surveyed area show recent activity up until the presumed 1883 deposits. Several buried and thus older deposits of similar thickness are imaged, sandwiched in between what is inferred to be hemipelagic sedimentation. The uppermost sediments are dominated by hemipelagic green muds with little organic matter and high ash content. Intercalated turbidite and volcanic ash layers are frequent. Modern sedimentation is controlled by strong currents with evidence for both strong erosion in the west and areas of focused deposition in the east of the archipelago. The seismic data show widespread occurrence of gas and water column imaging reveals active venting from the seafloor in numerous locations.

The bio-optical measurements of the surface water and the water color along the transect provided high-resolution datasets of important oceanographic parameters, such as salinity, water turbidity, and color as well as phytoplankton biomass. They showed comparatively constant conditions along the transect, as is typical for the nutrient-poor, open areas of the ocean. Due to the high frequency of the data acquisition, the physiological effect of the light adaptation of the phytoplankton could also be observed using the fluorescence data collected.

1.2 Zusammenfassung

Die Fahrt SO299/2 des deutschen Forschungsschiffes SONNE war eine Transitfahrt mit vier Arbeitstagen. Der wissenschaftliche Schwerpunkt lag auf dem Krakatau-Archipel in der Sundastraße, der Quelle von mindestens zwei großen Tsunamis in historischer Zeit. Reflexionsseismische Profile, hydroakustische Daten und Sedimentkerne wurden westlich, südlich und östlich der Inselgruppe gesammelt. Darüber hinaus wurden auf einem Transekt von Singapur nach Mauritius biooptische Beobachtungen zur besseren Charakterisierung und Parametrisierung des Unterwasserlichtfeldes im Indischen Ozean durchgeführt.

Ziel der Krakatau-Untersuchung war es, die eruptierten Volumina der katastrophalen Eruption von 1883 zu erforschen und die Prozesse zu entschlüsseln, die zu einem zerstörerischen Tsunami führten. Die seismischen Aufnahmen zeigen drei seismisch unterschiedliche Arten von Ablagerungen, die möglicherweise von den Ereignissen von 1883 herrühren, da sie sich in der Nähe des modernen Meeresbodens befinden. Sie variieren in ihrer Mächtigkeit und erreichen stellenweise bis zu 100 m. Eine der Ablagerungen wird von großen Blöcken mit Durchmessern von bis zu 400 m gekrönt, die bis zu 30 m aus dem umgebenden Meeresboden herausragen. Die Größe und Dichte der Blöcke nimmt mit zunehmender Entfernung zum Vulkan ab, was eher auf eine Ablagerung von Schuttströmen als auf einen pyroklastischen Strom schließen lässt. Normale Verwerfungen, die sich über das untersuchte Gebiet erstrecken, zeigen rezente Aktivität bis zu den vermuteten Ablagerungen von 1883. Mehrere vergrabene und somit ältere Ablagerungen ähnlicher Mächtigkeit werden abgebildet, die zwischen einer vermutlich hemipelagischen Sedimentation liegen. Die obersten Sedimente werden von hemipelagischen Grünschlämmen mit wenig organischer Substanz und hohem Aschegehalt dominiert. Häufig sind Turbidite und vulkanische Ascheschichten eingelagert. Die moderne Sedimentation wird durch starke Strömungen gesteuert, wobei es Anzeichen für eine starke Erosion im Westen und Gebiete mit konzentrierten Ablagerungen im Osten des Archipels gibt.

Die biooptischen Messungen des Oberflächenwassers und der Wasserfarbe entlang des Transekts lieferten hochauflösende Datensätze wichtiger ozeanographischer Parameter wie Salzgehalt, Wassertrübung und -farbe sowie Phytoplanktonbiomasse. Sie zeigten entlang des Transekts vergleichsweise konstante Bedingungen, wie sie für die nährstoffarmen, offenen Bereiche des Ozeans typisch sind. Aufgrund der hohen Frequenz der Datenerfassung konnte anhand der erhobenen Fluoreszenzdaten auch der physiologische Effekt der Lichtadaption des Phytoplanktons beobachtet werden.

2 Participants

2.1 Principal Investigators

Table 2.1: Principal Investigators of SO299-2

Name	Institution
Urlaub, Morelia, Prof.	GEOMAR
Berndt, Christian, Prof.	GEOMAR
Karstens, Jens, Dr.	GEOMAR
Kutterolf, Steffen, Dr.	GEOMAR
Walter, Thomas, Prof.	GFZ
Wollschläger, Jochen, Dr.	ICBM
Zielinski, Oliver, Prof.	ICBM (now IOW)

2.2 Scientific Party

Table 2.2: Scientific Party of So299-2

Name	Discipline	Institution
Urlaub, Morelia, Prof.	Marine Geology / Chief Scientist	GEOMAR
Ardhyastuti Supardi, Sri	Coring	BRIN
Bartels, Thies	Seismic technician	GEOMAR
Belo, Julie, Dr.	Coring - Volcanology	GEOMAR
Berndt, Christian, Prof.	Seismic	GEOMAR
Berndt, Janiene	Data Management, Seismic	GEOMAR
Budi Nugroho, Adam	Hydroacoustics, Coring	BRIN
Furst, Severin, Dr.	Hydroacoustics	GEOMAR
Karima, Shofia	Seismic	BRIN
Klein, Elisa	Hydroacoustics	GEOMAR
Kühn, Michel	Seismic	GEOMAR
Matthies, Fiene	Hydroacoustics	GEOMAR
Meredew, Kerys	Coring - Volcanology	University of Birmingham
Pank, Katharina	Coring - Volcanology	GEOMAR
Petersen, Asmus	Coring technician	GEOMAR
Pratama, Aditya, Dr.	Seismic	BRIN
Preine, Jonas	Seismic, coring	Universität Hamburg
Suendra	OBSERVER	Indonesian Navy
Völsch, Ann-Marie	Seismic, coring, administration	GEOMAR
Voss, Daniela	Bio-optics	ICBM
Wollschläger, Jochen	Bio-optics	ICBM

2.3 Participating Institutions

BRIN	National Research and Innovation Agency (Indonesia)
GEOMAR	Helmholtz-Zentrum für Ozeanforschung Kiel
GFZ	Helmholtz-Zentrum Potsdam – Deutsches GeoForschungsZentrum
ICBM	Institute for Chemistry and Biology of the Marine Environment
	Indonesian Navy
	Universität Hamburg
	University of Birmingham

3 Research Program

3.1 Description of the Work Area

The main working area of cruise SO299/2 was the Krakatau archipelago in the Sunda Strait between Sumatra in the north and Java in the south. The archipelago consists of four uninhabited islands with the active volcano Anak Krakatau in its center. During SO299/2 the volcano's alert level was at 3, which required keeping a minimum distance of 5 km around the crater. The inner part of the archipelago is a nature protected area. Water depths in the working area are mostly below 150 m. North of Krakatau the water depth is below 25 m and was therefore not accessible to RV SONNE. Strong currents with speed of up to 3 kn prevail in the Sunda Strait, with a few areas of less currents probably due to shadowing effects of the islands of the archipelago. A transect across the Indian Ocean brought us from the Sunda Strait at 6°S to Mauritius at 20°S.

3.2 Aims of the Cruise

The main goal of the cruise was to gain a better understanding about the geological processes controlling volcanogenic tsunami genesis, and to investigate post-collapse material redeposition and erosion processes. Krakatau represents an excellent target, because it is possible to study tsunami source parameters for the explosive eruption in 1883 as well as for the sector collapse in 2018. There are detailed eyewitness accounts, tide gauge measurements, and onshore analyses of pyroclastic flow deposits for the 1883 eruption. Marine reflection seismic profiles covering the offshore deposits as well as the caldera allow closing significant observational gaps regarding the relative timing and magnitude of potential tsunamic processes during the course of the eruption and thus allow to reconstruct the genesis of the deadliest volcanogenic tsunami in history. Our understanding of the 2018 sector collapse of Anak Krakatau is mainly based on remote sensing and tsunami observations, while existing marine geophysical surveys could only reproduce the distribution of sector collapse blocks and the shallowest sediments within the caldera. However, the available data lack penetration depth to constrain the basal contact between the primary slide mass and the substrate, which are key controls of its emplacement dynamics. Based on the currently available source parameter constraints, existing post-collapse tsunami simulations for both events help little to understand basic geological processes during tsunami genesis. However, the new data will allow to characterize and quantify the most important source processes and therewith reach a step change in our understanding of the disastrous 1883 and 2018 events and volcanogenic tsunami genesis in general.

The general objective of the side-user activities was to investigate the inherent and apparent bio-optical properties of surface waters in the Indian Ocean and relate them with hydrographical parameters (e.g., temperature and salinity), fluorescence characteristics of the dissolved fraction of seawater and the characteristics of its particulate fraction.

3.3 Agenda of the Cruise

The original schedule of the cruise with four working days was compromised by the requirement to enter an Indonesian port to obtain work visa necessary to conduct research in Indonesian Waters. After customs and immigration clearance the scientific work started directly upon leaving the port of Bakauheni with hydroacoustic data acquisition during the transit to the

working area. A 26 hour long seismic survey with parallel acquisition of hydroacoustic data was followed by 14 hours of gravity coring and a second 18 hours long seismic survey. Both seismic surveys started during daylight. Scientists and nautical officers watched out for marine mammals one hour prior to the start of the airgun and during seismic profiling. Core sites were carefully selected to avoid areas marked as coral occurrence. All works were planned to avoid entering the nature protected area inside the archipelago. Because of ongoing volcanic activity at Anak Krakatau it was not possible to enter the caldera.

The transect from the Sunda Strait to Mauritius went smooth and all planned side-user activities as well as underway measurements were carried out without problems in international waters (Fig. 3.1).

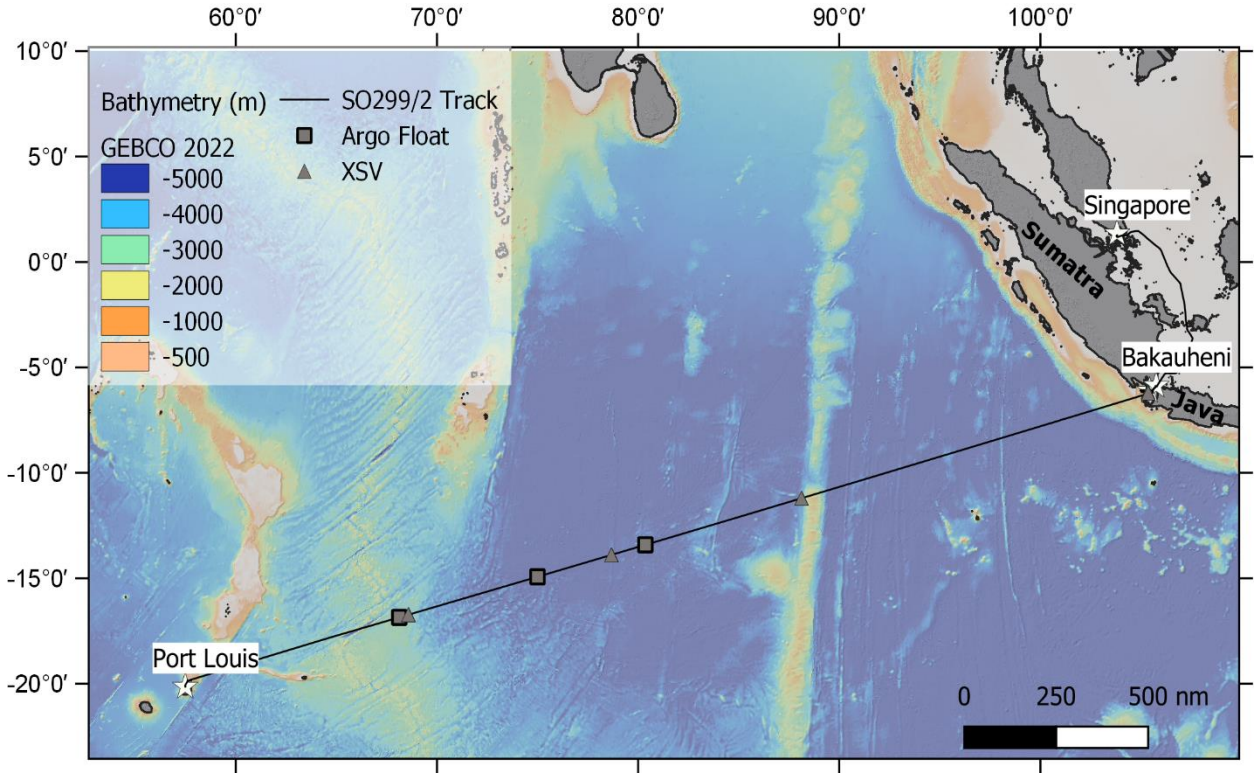

Fig. 3.1 Track chart of RV SONNE Cruise SO299/2. Bathymetry from GEBCO (2022). The main working area is nestled between the Indonesian islands of Java and Sumatra.

4 Narrative of the Cruise

On 14 August 2023, 16 scientists boarded RV SONNE via the Singapore Cruise Centre. Preparations in the laboratories started soon after. Work on deck was soon interrupted by heavy tropical rain, which lasted all afternoon.

The ship departed from Singapore in the morning of the 15 August and passed through the Strait of Singapore and into the South China Sea in calm sea conditions. Clocks were changed one hour back to GMT+7. The transit to Bakauheni on the southern tip of Sumatra (Indonesia) continued on the following day, 16 August. RV SONNE crossed the equator at 06:45 local time. Still on transit, a releaser test in 30 m water depth was conducted in the afternoon of the 17 August.

At 7:00 local time on 18 August 2023 RV SONNE arrived on anchorage at the ferry port of Bakauheni. In the morning four Indonesian scientists and one Indonesian observer boarded the

ship to stay on board during research activities in Indonesian Waters. Representatives of the Indonesian research agency BRIN, the agent and custom officers accompanied them. The passports were brought to the nearest immigration office for entry and visa stamps for Indonesia and arrived back to the ship in the evening.

At 11:30 on 19 August RV SONNE obtained clearance by Indonesian customs and immediately started sailing towards the working area. The three-hour transit was used for starting the hydroacoustic systems; the shallow water multibeam echosounder EM710 and the Parasound sediment echosounder, and for taking a vertical sound speed profile with an expendable meter. Upon arrival to the Krakatau archipelago in the early afternoon the scientists deployed the 75 m long streamer and one airgun for 2D seismic profiling in calm weather conditions. The wind picked up lightly in the evening.

The seismic survey continued until 16:00 of the next day, 20 August. After recovery of the seismic equipment, the ship moved to the west of the archipelago to conduct a Parasound survey for gravity core site selection until 19:00. The first gravity core station returned two empty corers (10 m and 5 m barrel) and the RV SONNE translated to the second core site. Here, at 22:00 local time the first sediment samples arrived on deck (full 5 m barrel). A second try with a 10 m barrel also recovered 5 m of sediment.

The coring program continued until the morning of the 21 August. The last gravity core with almost 8 m recovery was on deck at 7:00. Soon after the seismic streamer and airgun were deployed for the second survey again in calm weather.

Seismic profiling continued until 1:00 in the night of the 22 August, when the equipment was brought back on deck. RV SONNE sailed back to Bakauheni, where she arrived at 6:00 on anchorage. This was also the end of the main user scientific program. At 9:00 representatives of the German embassy in Jakarta and of BRIN visited the ship. Custom and immigration officers boarded the ship to process outward clearances. At 13:00 the visitors of the German embassy and BRIN and the four Indonesian scientists and observer left the ship to head back to land. At 22:00 RV SONNE was ready to depart from Bakauheni and start the transit to Port Louis across the Sunda Strait and the Indian Ocean.

No scientific work was conducted on the 23 August as the ship was sailing through Indonesian Waters.

On 24 August in the early morning the underway measurements started, which included seafloor mapping with the deep-water multibeam echosounder EM122, ADCP measurements, water sampling for salinity measurements and bio-optical properties as well as radiometer observations. All measurements were stopped in the evening to allow for transit through the Australian EEZ. Clocks were changed back by one hour to GMT+6.

On a bright and sunny 25 August after breakfast all underway measurements were started again and continued without disruption until the ship reached the EEZ of Mauritius.

On 26 August RV SONNE crossed the Ninety East Ridge and an XSV was deployed. In the evening, the first out of five Argo Floats was deployed at 87°E for the Australian Argo Program.

Underway measurements continued on the 27 August and the second Argo Float was deployed after lunch at 84°E. In the night to Monday the local time was changed to GMT+5.

The third Argo Float was brought out in the morning of the 28 August. Underway measurements continued. Argo Float number four was deployed on the 29 August 2023 at 7:30 board time. On Wednesday 30 August an expandable sound velocity profile was taken during transit and the vessel

crossed the Southwest Indian Ridge. The last Argo Float was deployed in the afternoon. All underway measurements were stopped in the evening of that day before reaching Mauritius waters.

The following two days were used for packing and cleaning the laboratories. At 9:00 local time on 2 September 2023 RV SONNE picked up the pilot and entered the port of Port Louis, where research cruise SO299/2 terminated.

5 Preliminary Results

5.1 Hydroacoustics

(E. Klein[1], S. Furst[1], F. Matthies[1], M. Urlaub[1], A. Budi Nugroho[2])

[1]GEOMAR, [2]BRIN

5.1.1 Multibeam bathymetry: System Overview and Data Processing

Instrumentation: Kongsberg multibeam echosounder systems are permanently installed on RV SONNE; the EM122 for full ocean depth and the EM710 system with a maximum acquisition depth of approximately 2000 m according to the manufacturer's data. Since the working area was mostly within water depths of <200 m only the EM710 was used. The EM122 was used on our transit across the Indian Ocean to acquire on-the-way data.

In addition to bathymetric information the EM122 and the EM710 system register the amplitude of each beam reflection. The amplitude signals correspond to the intensity of the echo received at each beam. It is registered as the logarithm of the ratio between the intensity of the received signal and the intensity of the output signal, which results in negative decibel values. Both systems also allow recording the entire water column. The water column data correspond to the intensity of the echoes recorded from the instant the output signal is produced. All echoes coming from the water column, the seabed and even below the seabed are recorded for each beam. The water column data were stored in separate *.wcd files.

Both the EM122 and EM710 systems apply beam focusing to both transmit and receive beams in order to obtain the maximum resolution also inside the acoustic near-field. The systems are capable of producing more than one sounding per beam (so-called high density mode), such that the horizontal resolution is increased and is almost constant over the whole swath. In multiping mode, two swaths are generated per ping cycle, i.e. one beam is slightly tilted forward and the second ping slightly tilted towards the aft of the vessel, resulting in double the amount of soundings. As a consequence, both systems achieve a footprint of 0.5° across cruise direction and 1° in cruise direction. High-density equidistant mode was used throughout cruise SO299-2.

External Trigger: Due to interference of the Parasound Sediment Echo Sounder in the multibeam data, the two hydroacoustic systems were externally triggered using the K-sync software designed by Kongsberg. For water depths <200m, a trigger cycle consisted of four signals to the EM710 and one to the Parasound. The multibeam echosounder is sending a feedback, when the data is coming in, so that the time per ping was variable. The Parasound does not have this function, thus it was given a set time of 750ms per trigger cycle. In two profiles with greater water depths, the trigger cycle was set to a single signal to each of the devices and the time of the

Parasound set to up to 2000ms to adjust for the longer travel time of the acoustic signal through the water column.

Positioning is implemented onboard RV Sonne with conventional GPS/GLONASS plus differential GPS (DGPS) by using either DGPS satellites or DGPS land stations resulting in quasi-permanent DGPS positioning of the vessel. The operator station with the Seafloor Information Sytem (SIS) acquisition software receives these signals. Ship motion and heading are compensated within the Seapath and SIS by using a Kongsberg MRU 5+ motion sensor.

Kongsberg EM710: The high-resolution shallow water multibeam echosounder transmits signals in the 70-100 kHz range. The system generates 256 beams providing 400 soundings. In multiping mode a maximum of 800 soundings per ping can be generated. The transmit fan is divided into three sectors to maximize range capability, but also to suppress interference from multiples of strong bottom echoes. The sectors are transmitted sequentially within each ping, and use distinct frequencies or waveforms. The maximum opening angle is 140°. During SO299-2 the EM710 generally delivered high-quality data between 50 m to approximately 1000 m water depth and worked reliably. As the weather was good, we were aiming for maximum coverage and chose the maximum opening angle of 140°.

Sound velocity: Beamforming requires sound speed data at the transducer head, which is available from a Valeport MODUS SVS sound velocity probe. The probe is located in centre of the vessel below the keel, and hence in the direct vicinity of the transducers. This signal goes directly into the SIS operator station.

Vertical sound velocity profiles were acquired with expandable sound velocimeters from Lockheed Martin. These consist of an expendable probe, a data processing/recording system, and a launcher. An electrical connection between the probe and the processor/recorder is made when the canister containing the probe is loaded. Following launch, a thin copper wire de-reels from the probe as it descends vertically through the water. As soon as an electrode within the nose of the expendable probe makes contact with the water, the circuit is complete and sound velocity data is sent to the ship-board data processing equipment. Data are recorded and displayed in real time within the WinMK21 software as the probe falls. The resulting .edf files were converted into .asvp format in order to be readable by the EM122 and EM710.

Post-processing: For multibeam post-processing and visualisation we used the software Qimera developed by QPS hydrographic and marine software solutions (http://www.qps.nl/display/main/home). When loading data from Kongsberg systems into Qimera, the software checks the detection class “show flag” to determine if soundings are accepted or rejected. Class 8 will be rejected by default, as recommended by the manufacturer. Qimera then launches any required processing and applies a weak filter to eliminate outliers to all loaded data. The soundings were then cleaned manually for further elimination of erroneous soundings.

5.1.2 Parasound: System Overview and Data Processing

Method: RV Sonne is equipped with an Atlas Parasound DS P-70 parametric deep-sea sediment echosounder for full ocean depth. The system is a narrow beam sediment echosounder (opening angle 4.5° x 5.0°) that utilises the so-called parametric effect to generate a very low frequency secondary signal by emitting two primary signals of higher frequencies. The Parasound system transmits two independent pulse-modulated harmonic signals via the same transducer array. To generate and utilise the parametric effect these signals must be generated with extremely high amplitudes. At such signal levels the seawater does not only serve as a propagation medium for the original signals but also generates additional new signal components at different frequencies. During SO299-2 the primary frequencies were 18 kHz and 22 kHz. The resulting secondary frequencies are 4 kHz and 40 kHz. For sediment penetration in particular the secondary low frequency is of interest. In the working area around the Anak Krakatau Archipelago the system emitted a rectangular frequency modulated single pulse. The receiver band width for both high frequencies was 66 % and for both low frequencies 33% of the output sample rate (12.2 kHz). The sound velocity was manually set to 1500 m/s.

Processing: All raw data were stored in the ASD data format (Atlas Hydrographic), which contains the data of the full water column of each ping for all four frequencies as well as the full set of system parameters. Additionally, a 100-150 m-long reception window centred on the seafloor of the primary high and the secondary low frequencies was recorded in the compressed PS3 data format after resampling the signal back at 12.1 kHz. This format is in wide usage in the PARASOUND user community and the limited reception window provides a detailed view of subbottom structures. All data were converted to SEG-Y format during the cruise using the software package ps32sgy version 15.9 (Hanno Keil, Uni Bremen). The software re-fits the different time windows and allows generation of one SEG-Y file for longer time periods. In this format the seismic interpretation software IHS Kingdom can easily read and display the Parasound data.

5.1.3 Preliminary results

The hydroacoustic measurements were conducted parallel to the 2D seismic survey, for the identification of sediment core locations, as well as during transits between stations.

Even though we did not conduct a dedicated multibeam survey and the coverage of the working area was limited due to narrow swaths in very shallow water, the data is of high quality and preliminary observations can be made (Fig. 5.1.1).

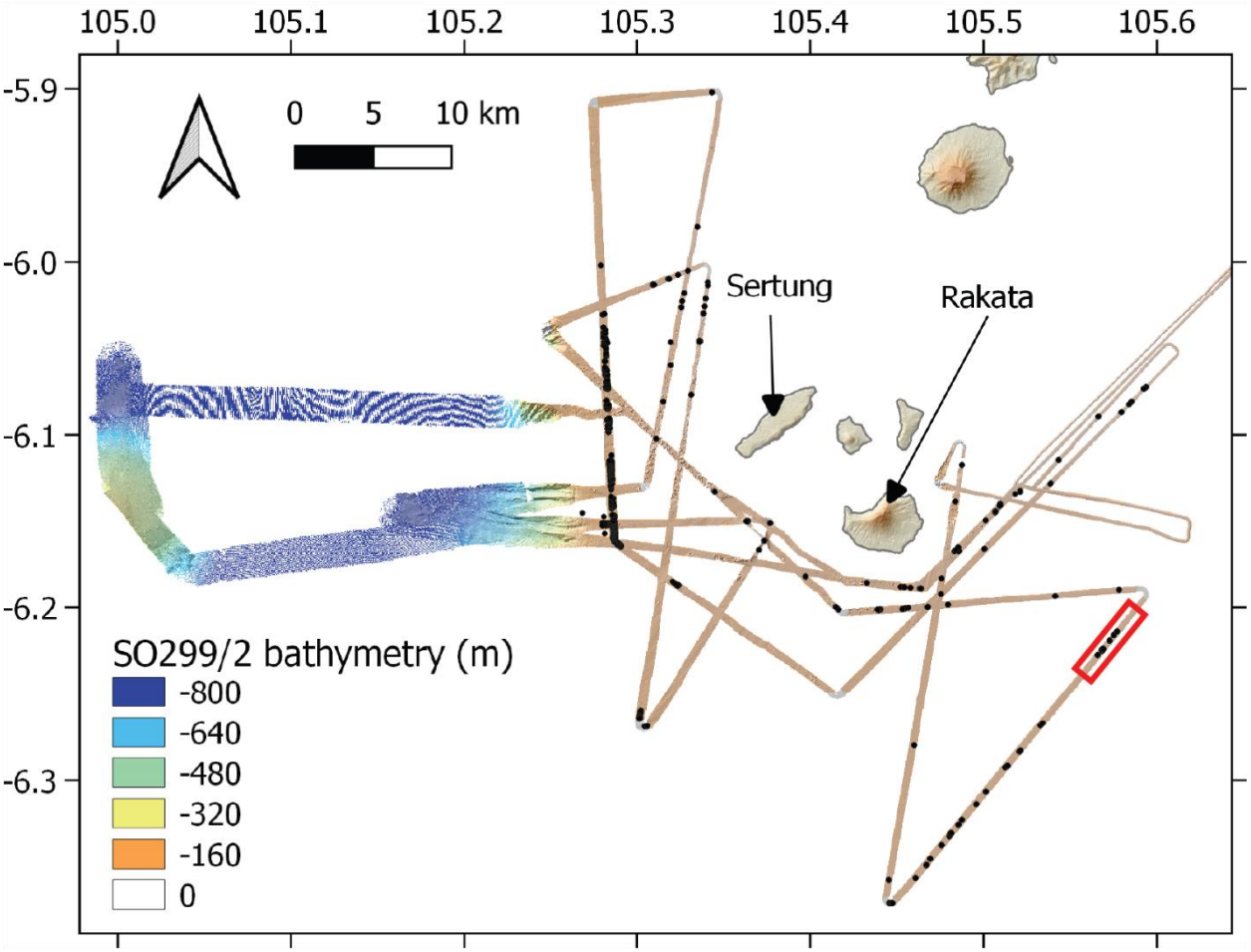

Fig. 5.1.1: Swath bathymetric data acquired with the EM710 in the main working area. Grid spacing is chosen to optimally represent sounding density in water depths <300 m. The density of soundings in deeper water is insufficient so that gridding artefacts occur. The black dots show locations where water column anomalies were identified. The red square shows the location of the example in Fig. 5.1.3. The anomalies are probably caused by gas rising from the seafloor.

The seafloor south and south-west of the archipelago is mostly flat with water depths ranging between 70 m and 130 m. It is slightly inclined towards the west, where two profiles cross an escarpment deeply incised by gullies. Above the escarpment, a few SW-NE striking linear incisions are visible. These are likely caused by the strong currents in this area. North-west of the volcanic archipelago, blocks of up to 300 m lateral extension and 30 m elevation above the surrounding seafloor are visible. Their lobe-shaped, surficial position suggest the emplacement in a geologically recent mass wasting event, most likely during the 1883 eruption. Deposition during the 2018 collapse of Anak Krakatau can be excluded because the blocks are visible in swath bathymetry data acquired during cruise SO137 in 1998 (Fig. 5.1.2) (Reichert 1998, https://webapp-srv1a.awi.de/eBathy/cruise_info2. php?cruise=447). Additional to the proximal area which was the focus of the research, we acquired two profiles in W-E orientation, crossing the escarpment and an up to 1150 m deep basin west of the archipelago while exploring possible distal coring locations.

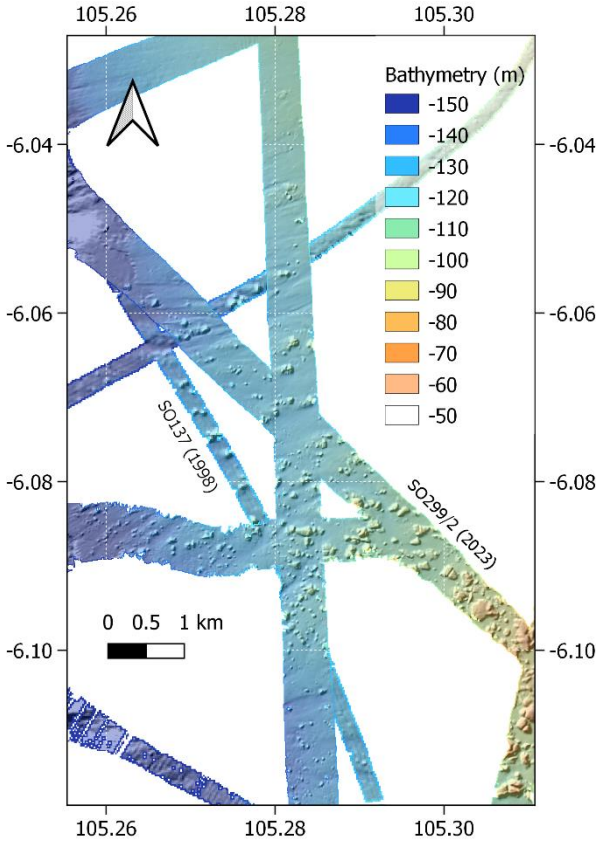

Fig. 5.1.2: Blocks scattered at the seafloor west of the island of Sertung in data acquired by RV SONNE in 1998 (narrow stripes) and in 2023 (wider stripes).

Table 5.1.1: Hydroacoustic surveys during SO299-2

	Date	File numbers	Ship speed
Transit to Krakatau	19 Aug 2023	01-05	10-12 knts
2D seismic profiling	19/20 Aug 2023	06-71	3-5 knts
Coring recon West	20 Aug 2023	72-78	8 knts
Transits Coring	20/21 Aug 2023	79-109	10 knts
2D seismic profiling	21/22 Aug 2023	110-153	3-5 knts
Transit to Bakauheni	22 Aug 2023	153-163	10-12 knts

The software FMMidwater reads, converts, and displays water column data. For fast screening of the water column data set we converted the data using a data point reduction factor of 4 and visually inspected the lines in the stack view. The water column images were analysed for anomalies in the water column that are caused by gas rising up from the seafloor. The water column images showed several anomalies of varying shapes, sizes, and abundances (Fig. 5.1.3).

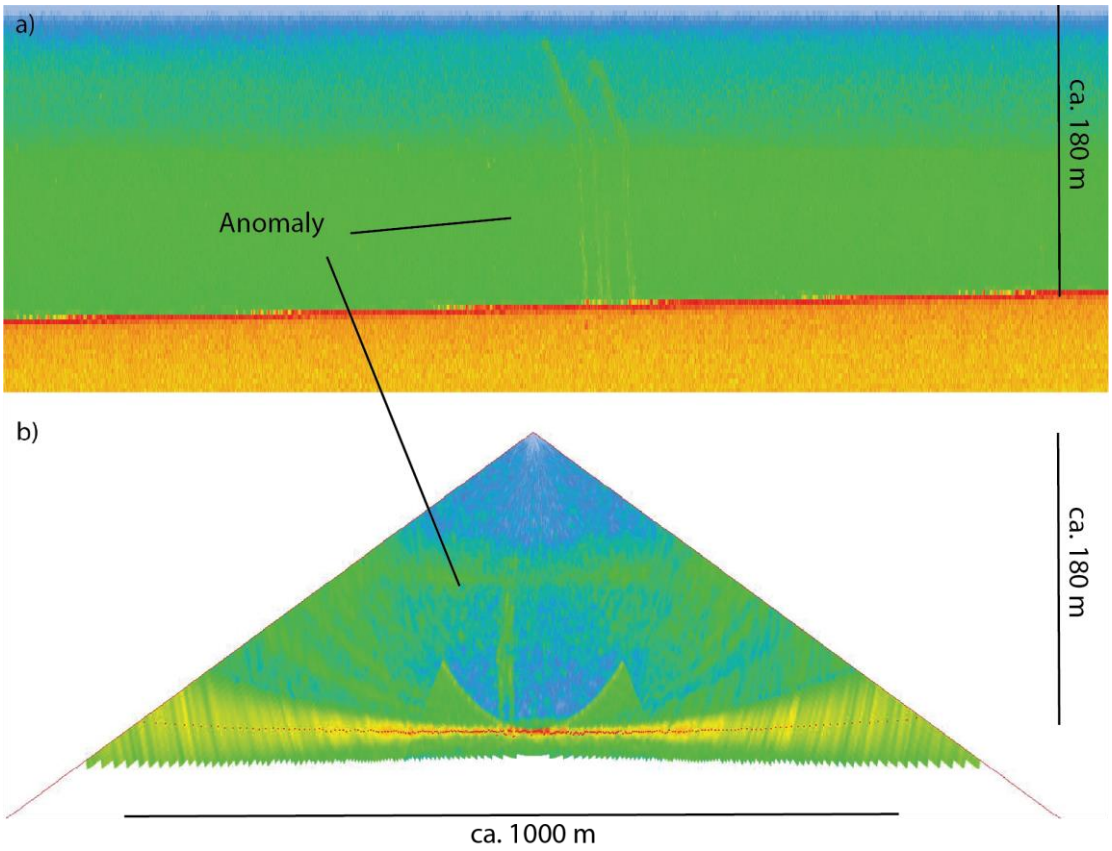

Fig. 5.1.3: Screenshots from the FMMidwater software showing an example of water column anomalies in the south-east of the Krakatau Archipelago. a) Stacked fans along the ship's track and b) water column image of one ping.

During the main survey at Anak Krakatau three sound velocity probes were launched on the 19th, 20th and 21st of August 14:00 local time. During the transit towards Mauritius three additional probes were launched, the second of which was compromised due to strong winds. The results are shown in Figure (5.1.4).

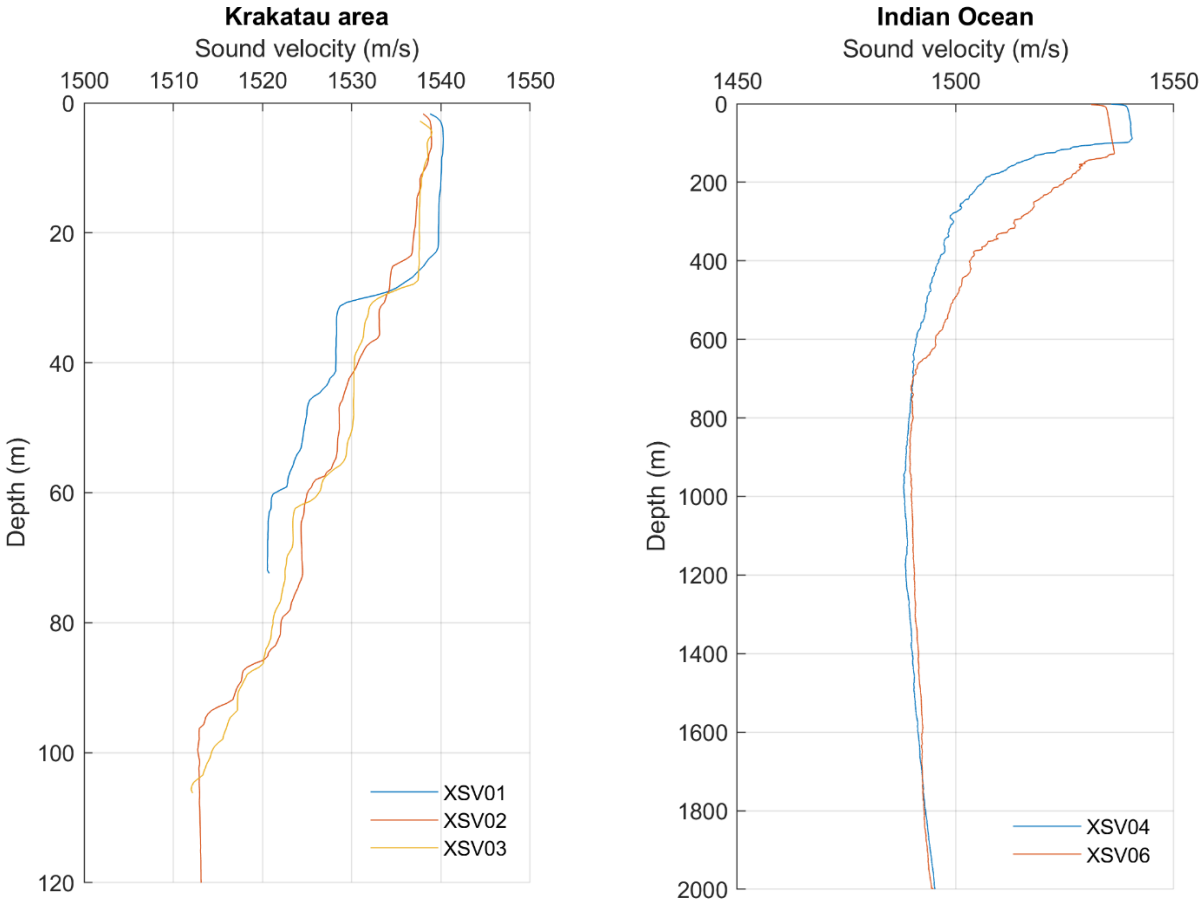

Fig. 5.1.4: Sound velocity profiles taken with XSVs; right: Krakatau area, left: Indian Ocean

The Parasound data is of high quality and data were recorded in parallel with the 2D seismic survey, for coring location reconnaissance and during transits. Areas of common dominant acoustic facies are visible in the data. Fig 5.1.5 shows an overview. In the west of the archipelago (Figure 5.1.5b) large blocks are visible. This layer thins out towards the north-west, where the penetration increases and stratified layers are visible beneath. In the north, the penetration is limited due to an abundance of gas (Figure 5.1.5c). In large areas in the south the Parasound is achieving little penetration. An exception is the area in the east, where a thick sequence of well-stratified layers are visible (Fig. 5.1.5d).

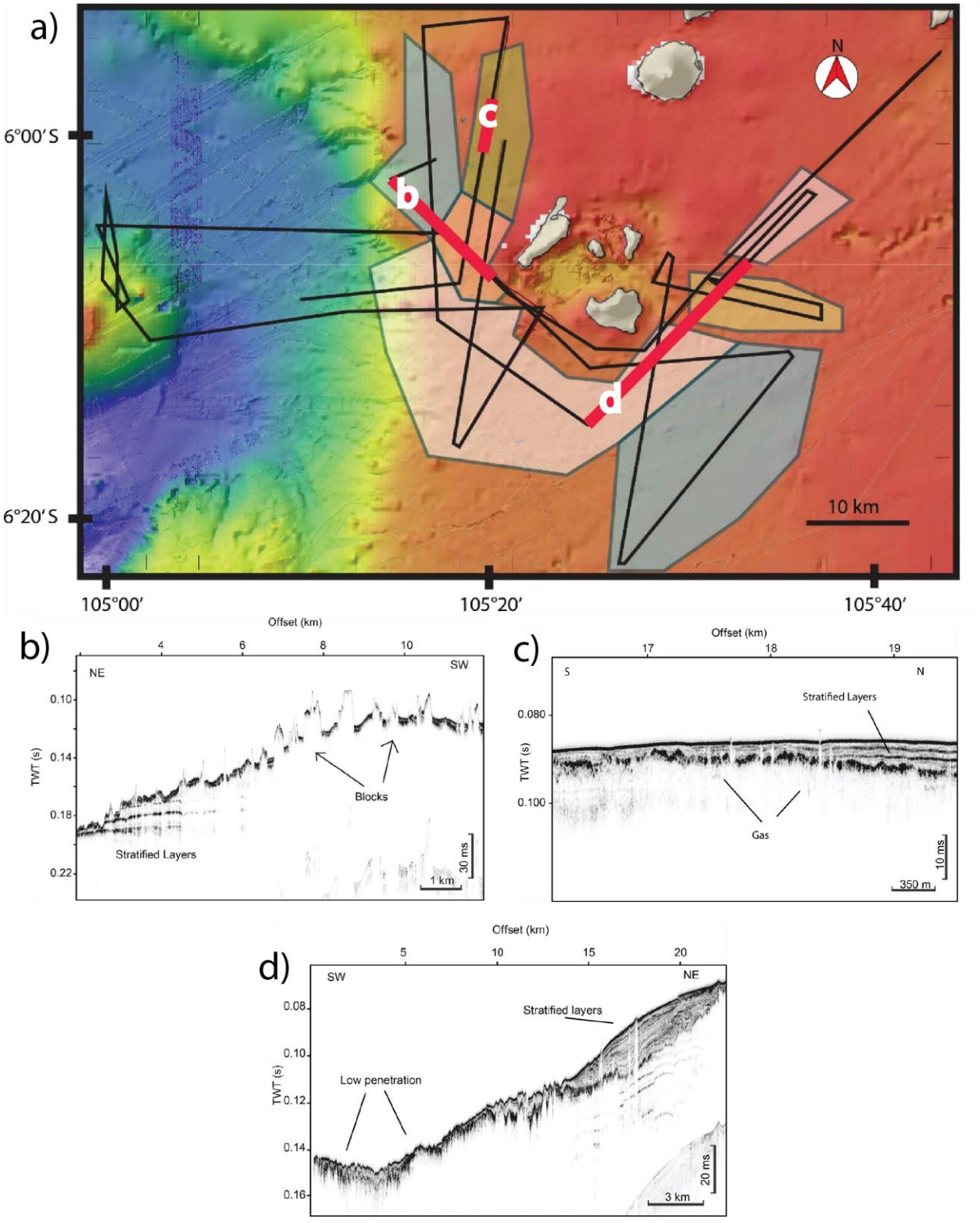

Fig. 5.1.5: **(a)** Overview of the Parasound data: black lines indicate the Parasound profiles, the positions of the figures in this report are highlighted in red. The colored polygons indicate areas of similar dominant acoustic facies in the Parasound data; White: low penetration, orange: large blocks, blue: chaotic facies, yellow: thick stratified layers.

5.2 2D Seismics

5.2.1 Seismic acquisition

(C. Berndt[1], M. Kühn[1], J. Preine[2], J. Berndt[1], A. Völsch[1], S. Karima[3], Pratama, A.[3])
[1]GEOMAR, [2]Universität Hamburg, [3]BRIN

During SO299/2 we used a high-resolution 2D seismic system to image the shallow subsurface at high resolution. The seismic source consisted of a single GI gun with 75/75 cubic inch generator and injector volumes, respectively. This array was towed 20 m behind the vessel at 2 m depth (Fig. 5.2.1). The air pressure was 140-145 bar. The shot interval was 5 s and the record length for each shot was 4.5 s.

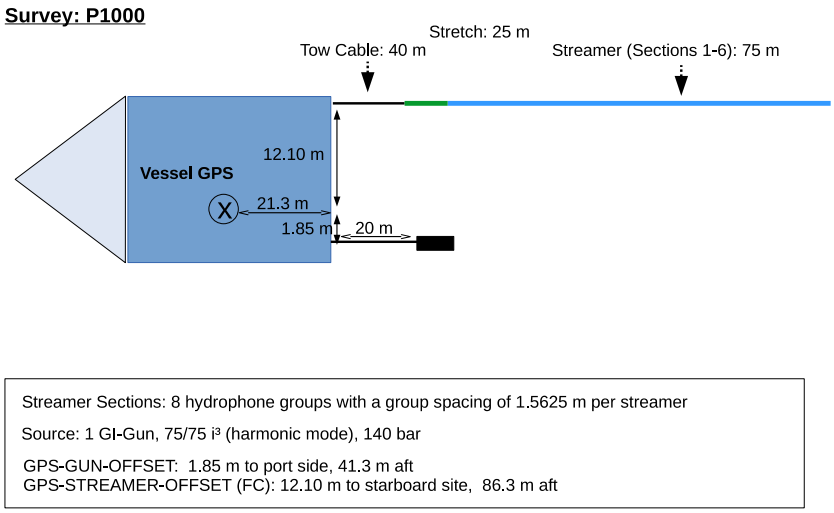

Fig. 5.2.1: Survey geometry for 2D seismic acquisition during SO299/2.

The seismic receiver consisted of a 40 m-long tow cable, a 25 m-long stretch section, a 75 m-long active cable and a 20 m-long line to the tail buoy. A weight was attached to this line 2 m before the tail buoy to keep the streamer at depth. The active cable comprised six sections of oil-filled Geometrics Geoeel streamers with 48 channels in total. The hydrophone group spacing was 1.5625 m. The streamer was towed without birds but visual inspection suggested that the streamer was towed between 0.5 and 1.5 m depth. The seismic data were A/D converted within digitizing bottles within each streamer segment and transferred to the ship using an ethernet network. The data were recorded with an SPSU and Geometrics software in SEG-D format.

For navigation we mounted a GPS antenna on the ship's superstructure close to the stern of the vessel. The position of this GPS antenna was measured with a tape measure and related to the towing points of the airgun source and the streamer. The navigation data were logged in parallel to the seismic data.

Seismic operations included two stations (SO299/2-2 and SO299/2-10) that covered 200 and 181 line kilometers, respectively (Fig. 5.2.2). Seismic operations were continuous and without any

downtime. Before each of the two surveys we conducted a visual inspection of the surroundings for marine mammals and as there were no mammals in sight operations started without delay. As there was only one air gun at low pressure a ramp up procedure was neither possible nor necessary. The watch keeping officer on the bridge was instructed to watch out for marine mammals during the surveys to allow emergency shut downs in case mammals would come closer than 500 m to the vessel. We only observed one mammal on the last day of the survey but it was too far away (> 2 km) to be identified and operations continued without interruption.

Onboard processing consisted of shot and receiver location calculation using the GPS navigation and the measured survey geometry (Fig. 5.2.1). The seismic data were than merged with the calculated shot and receiver locations. We determined the delay to be 150 ms throughout the survey and took this into account during processing. In the following we applied a frequency filter limiting the bandwidth of the data to 35-55 and 350-450 Hz. This was followed by a normal moveout correction with water velocity (1530 m/s, derived from CTD measurement) and stacking at 1.5625 m bin size along 18 profiles (P1001 to P1018). For imaging we used a Stolt migration with 1500 m/s velocity. The data were than exported to SEG-Y and loaded into KingdomSuite for quality control and preliminary interpretation.

5.2.2 Preliminary results

The seismic data are of high quality and do not show significant noise apart from a bubble pulse and the seafloor multiple (Fig. 5.2.3 and 5.2.4). Due to the relatively soft seafloor both these noise sources do not affect the imaging in a significant way, but it will be useful to suppress the seafloor multiple with more sophisticated processing as the data show clear evidence of primary reflections below the onset of the first seafloor multiple (Fig. 5.2.4). The penetration of the seismic data is generally good reaching more than 1 s two-way travel time in some parts of the survey area.

The 2D seismic data reveal a complicated pattern of various volcanogenic sedimentary deposits around the Krakatau archipelago. Fig. 5.2.3 shows an example of the distal parts of the deposits south of the archipelago. Some of the deposits are internally transparent and have a flat surface whereas others are characterized by high-amplitude internal reflections and a rough or hummocky surface. Others again are characterized by a dense field of blocks in an otherwise transparent matrix (not shown). The data will allow mapping of these deposits. Comparison with volcanogenic landslide deposits elsewhere will constrain the nature of these deposits and their emplacement processes.

Safety concerns (Krakatau was on alert level 3 throughout the survey) prevented us from collecting data inside the caldera. Nevertheless, the 2D seismic data hold ample information on the volcanic edifice of Krakatau before the 1883 collapse as some lines cross close to the foot of the edifice. They show laterally confined volcanic units that presumably consist of lava flows and ash deposits similar to modern Anak Krakatau. They are onlapped by 10s of meters-thick volcanogenic mass transport deposits that tend to be more chaotic near the top and more transparent at the base (Fig. 5.2.4).

Most lines show evidence for extensive normal faulting that has been active until the most recent geological past. The extensional tectonic regime has been reported earlier for the Sunda Strait (Susilohadi et al., 2009) and is corroborated by the new data.

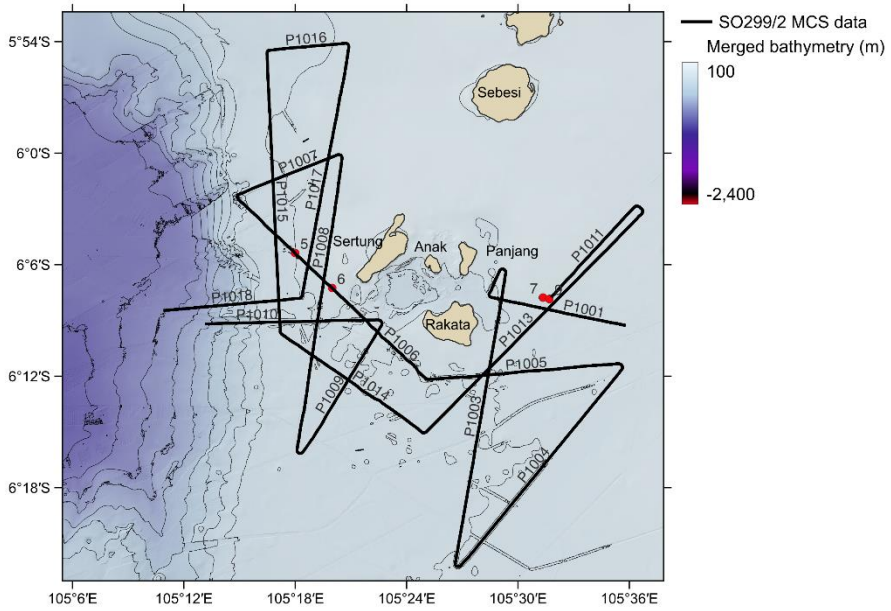

Fig. 5.2.2: Track chart for the 2D seismic lines collected during SO299/2. Altogether the survey covers about 380 line kilometers.

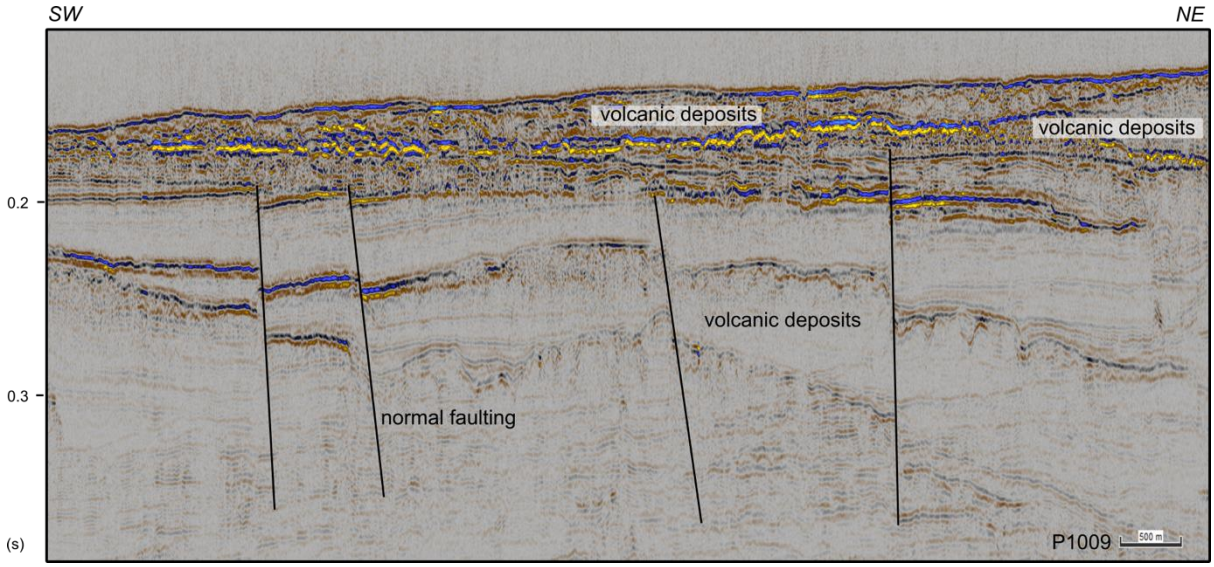

Fig. 5.2.3: Data example for the 2D multi-channel seismic data collected during SO299/2. The profile shows the character of the distal deposits of Krakatau and the strong tectonic overprint in the Sunda Strait that is offsetting the volcanic deposits into the most recent geological past.

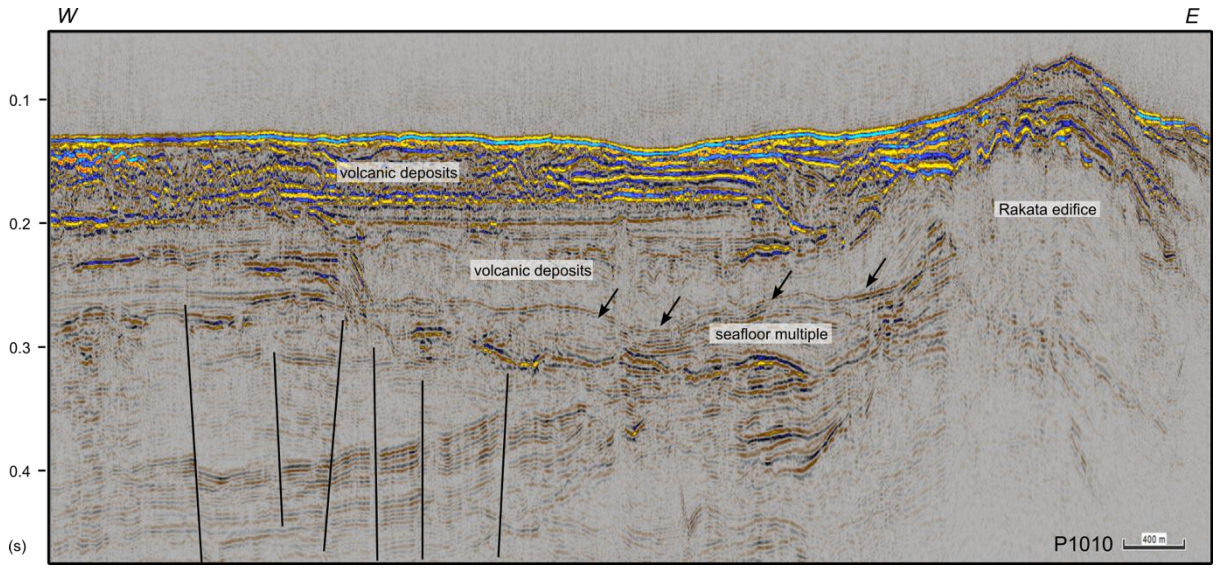

Fig. 5.2.4: Data example for the 2D multi-channel seismic data collected during SO299/2. The profile illustrates the proximal deposits that onlap the toe of Krakatau south of Rakata Island.

5.3 Gravity Coring

(J. Belo[1], K. Meredew[2], K. Pank[1], Ardhyastuti Supardi, S. [3])
[1]GEOMAR, [2]University of Birmingham, [3]BRIN

5.3.1 Introduction

Eruptive products of highly explosive volcanic eruptions generate buoyant eruption columns penetrating up to >20 km high into the atmosphere up to the level of neutral buoyancy where they spread laterally. Eruption clouds drift with the wind prevailing at any altitude and gradually drop their ash load over areas larger than 10s km². Collapses of eruption clouds produce devastating pyroclastic flows that can be widely distributed, and can travel far distances through and above water. Especially on oceanic islands the majority of the volcanic products is deposited in the marine environment. Wide aerial distribution across sedimentary facies boundaries, near-instantaneous emplacement, chemical signatures facilitating stratigraphic correlations, and the presence of minerals suitable for radiometric dating make ash layers excellent stratigraphic marker beds for marine geoscience. Marine tephrostratigraphy provides constraints on the temporal evolution of both, the volcanic source region and the ash-containing sediment facies, and is a good feature to correlate different sediment successions from on-land and marine environments with each other.

The Krakatau volcano is known for its paroxysmal caldera-forming Plinian eruption in 1883, which produced large amounts of rhyodacite pyroclastic deposits that have been deposited in the Sunda Strait and adjacent coastal regions, but also in far distal regions like the Cocos Islands (1,850

km away; Self, 1992). The eruption triggered a series of devastating tsunamis and resulted in the deaths of over 36,000 inhabitants (Umbgrove, 1928; Sudradjat, 1983). Krakatau volcano was a large oceanic volcanic island consisting of three NNW aligned active vents, Perboewatan (120 m), Danan (450 m) and Rakata (800m), which were largely destroyed by the 1883 eruption. The configuration of today's Krakatau Island complex can be attributed to probably two caldera-forming events, followed by the production of a new young volcanic island – Anak Krakatau (Fig. 5.3.1; Neumann van Padang, 1933; Sudradjat, 1983).

Volcanic activity within the Krakatau Island Complex initiated again in December 1927, with Surtseyan eruptions of basaltic andesitic magma originating approximately between the previous vents of Danan and Perboewatan (Umbgrove, 1928; Neumann van Padang, 1933). By August 1930, this continuous periodic activity resulted in the establishment of the new subaerial volcanic cone of Anak Krakatau (Neumann van Padang, 1983). Anak Krakatau's volcanic history can be separated into four broad phases: (1) 1927-1960, consisting of Surtseyan to Phreatomagmatic eruptions; (2) 1960-2018, the establishment of a fully subaerial vent, transition to Strombolian to Vulcanian eruptions and the initiation of lava flows; (3) 2018-2019, flank collapse and return to violent phreatomagmatic eruptions, rapidly rebuilding the island; and (4) 2019 – ongoing, the production of a new central cinder cone and subaerial vent producing new lava flows. Within these, three notable periods can be attributed to the thickest recorded on-land deposits of ash on the surrounding islands of Sertung and Panjang, termed 'burial-events' in reference to the widespread destruction of vegetation (Whittaker et al., 1989; Whittaker et al., 1992; Cutler et al., 2022). The first of which occurred in 1930-35, followed by activity in 1952-53 which resulted in up to 40 cm of ash 250 m from the shore of Sertung (Whittaker et al., 1989; Whittaker et al., 1992). It is also likely that other later periods, such as activity in the 1970s-80s, can also be attributed to thick on-land ash deposits and the destruction of vegetation, however records of first-hand observations are significantly limited. The final notable period of ash fall is directly following the December 2018 collapse of Anak Krakatau, in which ~25 cm of ash was deposited on Panjang, approximately 4 km away from the vent (Cutler et al., 2022).

Excluding Anak Krakatau's immediate post-collapse eruptions, recent volcanic activity is typically characterized by Strombolian to Vulcanian eruptions of basaltic andesitic magma, producing up to 3 km high eruption columns and effusions of localized lava flows (Gardner et al., 2013; Abdurrachman et al., 2018; PVMBG, 2022).

Tephra samples recovered from gravity cores during SO299/2 will be studied in detail to unravel the volcanic history of Krakatau volcano.

5.3.2 Methods

In total, nine sediment cores were taken by gravity coring during cruise SO299/2 in the vicinity to the Krakatau archipelago (Fig. 5.3.1). Seven successful attempts recovered between 2.65 m and 7.88 m sediments, while two attempts failed. The gravity corer (GC) was equipped with a 1.6-t-weight attached to the top of a 5- or 10-m-long steel tube enclosing an inner PVC tube. As soon as the cores arrived on deck, they were cut into approx. 1-m-long segments. The sediment cores

were split into halves, one for BRIN and the other for GEOMAR, following the agreement with the Indonesian research institute and government. The Indonesian colleagues wrapped and packed their core halves without sampling. The GEOMAR halves were described by means of sedimentological characteristics based on Munsell Color Chart and IODP (International Ocean Discovery Program) lithology classification and sampled for further petrographical and geochemical analyses (porewater, sediments, and tephra; see table 1). Visual identification of tephra layers is easy when the volcanic ash forms mm to cm-thick distinct and undistorted layers. In ocean island settings, however, mass wasting processes redistribute ashes and therefore visual recognition in core sections can be difficult. Photographs of each core section were taken with a Canon EOS 600D. The core segments were then wrapped and stored in D-tubes at room temperature.

In total, 34.76m of sediment were recovered during cruise SO299/2.

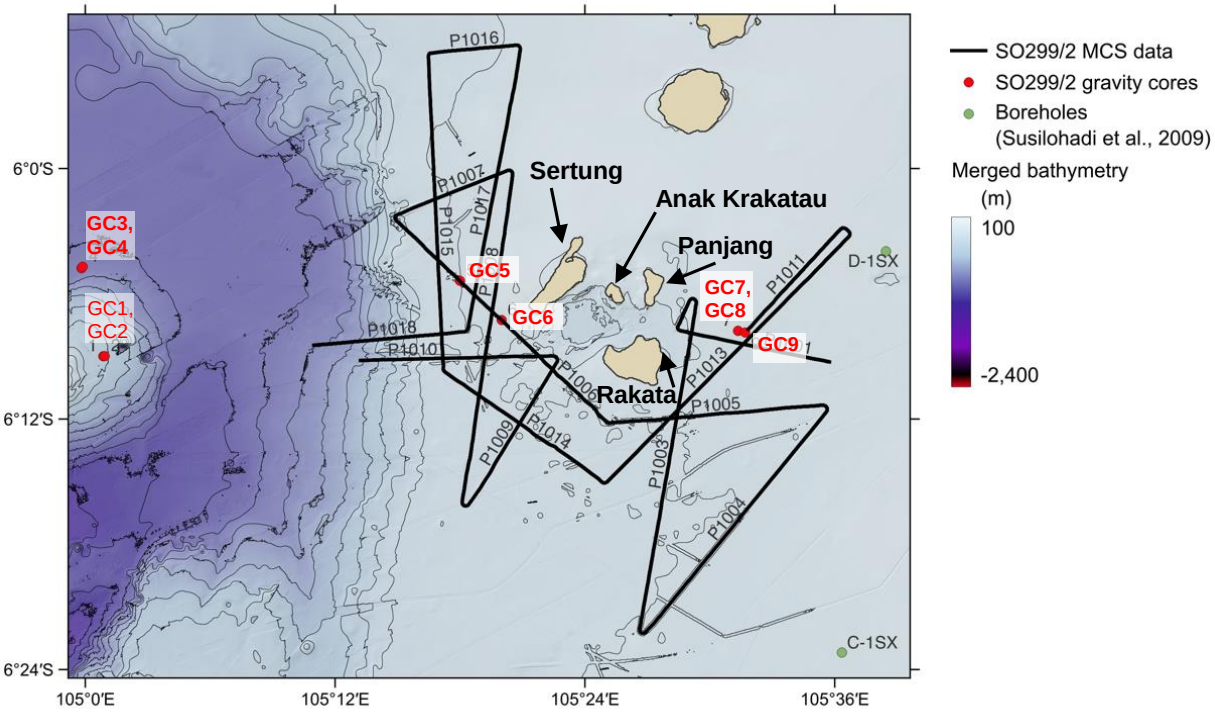

Fig. 5.3.1 Overview map of the working area. Black lines show Multi-Channel-Seismic (MCS) survey. Red circles mark coring locations of SO299/2-GC1 to -GC9.

5.3.3 Core descriptions

Location 1: Seamount west of Krakatau

At station SO299/2-4 (GC1 and GC2; Fig. 5.3.1) both attempts yielded no recovery.

Two attempts on the northern flank (SO299/2-5) of the seamount (Fig. 5.3.1) recovered two times 5 m sediments, the first attempt (GC3) with 5 m steel tube and the second attempt (GC4) with a 10 m steel tube.

The two cores are dominated by massive greenish-gray clay with few pyrite patches. The uppermost sediments were not recovered in GC3, but GC4 contains a ca. 20 cm thick fine to medium reversely graded white pumice lapilli layer in the uppermost part of the core, 8 cm below seafloor (cmbsf) (Fig. 5.3.2). Another 2 cm thick disturbed fine ash layer was recovered in GC3 at 158-160 cmbsf.

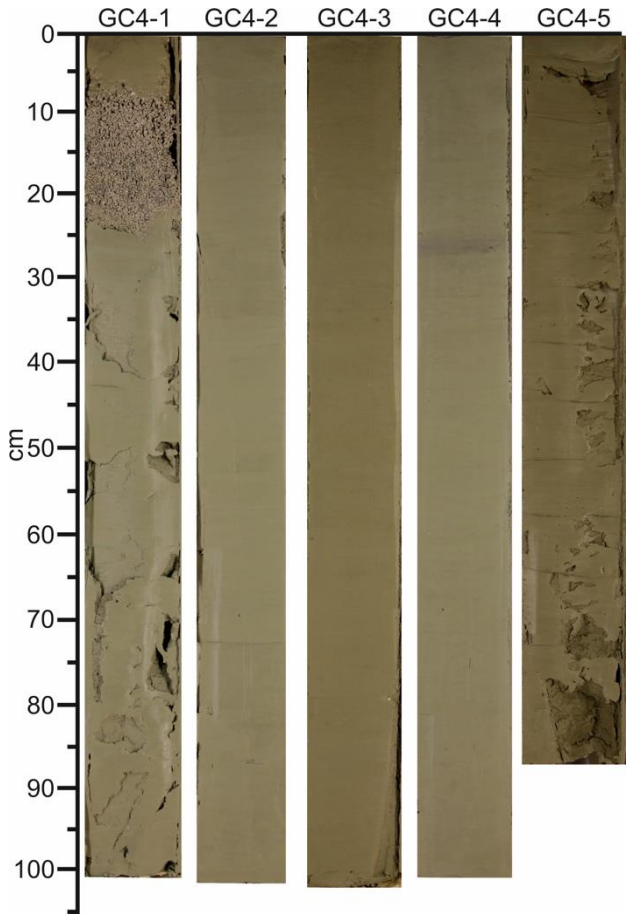

Fig. 5.3.2: Core composite of GC4. In the uppermost part of the core a reversely graded pumice lapilli layer was recovered.

Location 2: Block field west of the Krakatau caldera

To determine the lithology between the blocks that are distributed over large areas west and southwest of the Krakatau archipelago, we chose two coring locations (SO299/2-6 GC5 and SO299/2-7 GC6) between large blocks. For both locations we used 5 m steel tubes. Gravity core GC5 yielded 2.65 m recovery, and gravity core GC6 4.24 m of sediments.

GC5 is dominated by massive silty clay with dispersed ash. The upper section is heavily disturbed and soupy. There is one ash pod at 54-55 cmbsf and two ash layers at 99-106 cmbsf and 127-130 cmbsf. The lower layer is a disturbed pod layer of coarse dark ash and white fine pumice lapilli. The upper layer is a massive black medium ash layer with a diffuse lower boundary and a sharp, inclined top.

Gravity core GC6 is also dominated by massive silty clay with dispersed ash, with an overall downward increasing amount of ash and the appearance of fine to medium white pumice lapilli (Fig. 5.3.3). The grainsize increases from silty clay to sandy silt. The uppermost 24 cm are heavily disturbed and soupy. There are several ash layers or ash pods. A distinct layer is observed at 52-60 cmbsf, which is a slightly stratified coarse ash with diffuse, irregular boundaries. There is a coarse ash pod at 74-76 cmbsf, and another distinct medium ash layer with diffuse and disturbed boundaries at 85-93 cmbsf. Fine and medium angular white pumice lapilli are observed at 172-174 cmbsf, 188-189 cmbsf, 312-314 cmbsf, and 390 cmbsf. At 398-400 cmbsf there is a lense of white fine pumice lapilli (Fig. 5.3.3).

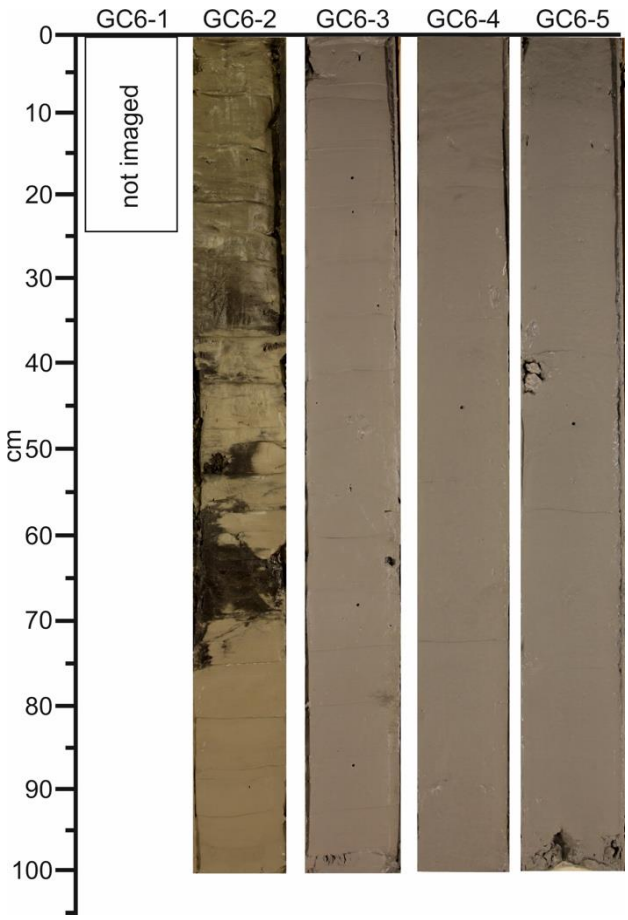

Fig. 5.3.3: Core composite of GC 6 with dark ash layers in the upper part of the core. Towards the lower part of the core the amount of ash increases and medium white pumice lapilli occur sporadically.

Location 3: East of the Krakatau caldera

Three gravity cores were taken at two stations in the east of the caldera to characterize the deposits in this region. Two cores were taken at the same location SO299/2-8, GC7 with a 5 m steel tube, and GC8 with a 10 m steel tube, but recovery was 5 m sediment for both attempts.

At station SO299/2-9 GC9 7.88 m of sediment were recovered with 10m steel tube.

The two gravity cores at SO299/2-8 are dominated by greenish-gray massive clayey silt and silty clay with ash and pumice lapilli pods. In GC7 there are pods and lenses at 20-21 cmbsf, 48-51 cmbsf, 72-74 cmbsf, 124 cmbsf, 180 cmbsf, and 364-368 cmbsf. There is a subtle color change

at 255 cmbsf. In GC8 there are thin dark layers in the upper 10 cmbsf, which might be ash. Another distinct medium-coarse ash layer occurs between 18-20 cmbsf, which is soupy and disturbed. There are pumice lenses at 70 cmbsf, and 82 cmbsf. At 144 cmbsf and at 147 cmbsf there are two coarse ash to fine white pumice lapilli layers with erosive contacts. Another pumice lapilli lense is observed at 162-164 cmbsf, the pumice lapilli are subrounded.

The amount of dispersed ash, ash pods, and pumice lapilli increases from 300 cmbsf downwards.

GC9 is also dominated by greenish gray patchy, slightly laminated (0-288 cmbsf) and massive (288-788 cmbsf) silty clay with dispersed ash (Fig. 5.3.4). There is a thin ash layer at 2 cmbsf, and a dark coarse ash layer at 9-11 cmbsf, which has irregular and disturbed boundaries. Pumice lapilli lenses are observed at 147 cmbsf and 170 cmbsf. There is an ash-rich horizon at 302-304 cmbsf, a black ash lense at 375-377 cmbsf, and more ash and pumice lapilli lenses at 429, 440, 458, and 530 cmbsf. At 539-542 cmbsf there is a pumice lapilli layer with white angular pumices mixed with dark ash. Another distinct dark medium ash layer is observed at 561-565 cmbsf. At 650-659 cmbsf there are erosive contacts and a grainsize increase to sandy silt with some fine pumice lapilli.

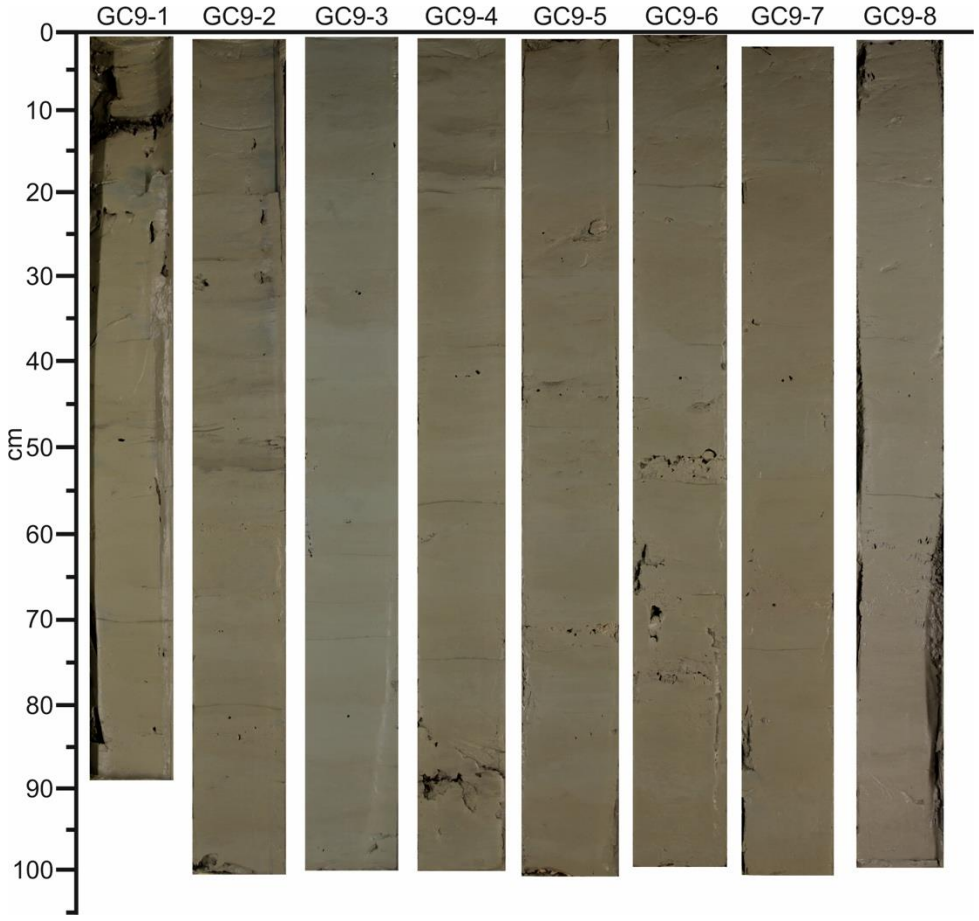

Figure 5.3.4: Core composite of GC9 with dark ash layers in the upper part of the core (section GC9-1) and increasing amounts of ash and pumice lapilli in the lower sections.

Table 5.3.1: Sample list for porewater, sediment geochemistry, and tephra:

GC #	sample depth porewater and sediment [cm]	sample depth tephra [cm]
SO299_2-4-2-GC2		CC
SO299_2-5-1-GC3		158-160
SO299_2-5-2-GC4		10-12
		326-328
SO299_2-6-GC5	90	54-55
	104	102-104
	130	129-131
	155	
SO299_2-7-GC6	114	24-26
	140	57-58
	190	75-76
	270	88-90
	370	172-174
	90	219-220
		243-244
		284-285
		299-300
		364-365
		399-400
		413-414
SO299_2-8-1-GC7	130	Top
	170	20
	30	49-50
	70	72-73
	45	84
	330	125
	370	133
	230	181
	270	467-468
	430	
	470	

GC #	sample depth porewater and sediment [cm]	sample depth tephra [cm]
SO299_2-8-2-GC8		18-19
		82
		142
		145
		160
		330-333
		357-358
		368
		383-384
		407-408
		455-457
SO299_2-9-GC9	50	2
	12	9-10
	120	147
	170	170
	220	302-304
	270	375-377
	330	411-412
	377	429
	430	458
	460	532-533
	530	539-542
	565	558
	630	561-563
	657	655-657
	730	760-762

5.4 Bio-optics

5.4.1 Objectives / Aims

The general objective of the proposed cruise is to investigate the inherent and apparent bio-optical properties of surface waters in the Indian Ocean and relate them with hydrographical parameters (e.g., temperature and salinity), fluorescence characteristics of the dissolved fraction of seawater and the characteristics of its particulate fraction. The proposed cruise transect of SO299-2 from Singapore to Mauritius is well suited for these investigations, as it crosses the main currents in the Indian Ocean, thus providing different water masses. The respective measurements were obtained by continuously measuring underway sensors that were installed on board, as well as from measurements on surface water samples taken from the ships seawater-system.

The general research aims of the proposed activities were the following: (i) Measuring the light field emerging from the water column (water leaving radiance and remote sensing reflectance) and combine point measurements from the ship with satellite observations to validate and improve processing algorithms for remote sensing reflectance and Ocean Color. (ii) Determination of bio-optical properties in the Indian Ocean and optical signatures of organic matter to develop a regionally applicable bio-optical parameterization. Further, the results will be compared with data from previous Sonne transects in the Pacific Ocean. (iii) Validation of sensors in the self-cleaning Monitoring Boxes (SMBs) on board RV SONNE as part of the quality control effort in the context of DAM (Deutsche Allianz Meeresforschung), as the ICBM is responsible for validation of the bio-optical (e.g. fluorescence) sensors. The proposed transect in international waters is perfectly suited to perform validation measurements for the sensors, which requires dedicated instruments and is thus not possible on every cruise. Respective measurements would support the delayed mode control of these optical sensors before publishing their data on the PANGAEA database.

5.4.2 Work performed during the cruise:

During the travel through international waters, several underway measurement systems obtained high resolution data sets. On the front of RV SONNE, a set of hyperspectral radiometers was installed. From these radiometric measurements, important apparent optical properties (the diffuse attenuation coefficient, remote sensing reflectance, Ocean Color) can be derived. Further, a FerryBox System (4H Jena, Germany) was connected to the ship’s seawater system to measure continuously biogeochemical parameters in the surface water (e.g., salinity, temperature, oxygen, turbidity, and chl-a fluorescence). To a bypass of the FerryBox, additional instruments, e.g. measuring optical transmission and nitrate, were connected. This bypass offers further the possibility to sample the surface waters daily in defined intervals for further lab analysis.

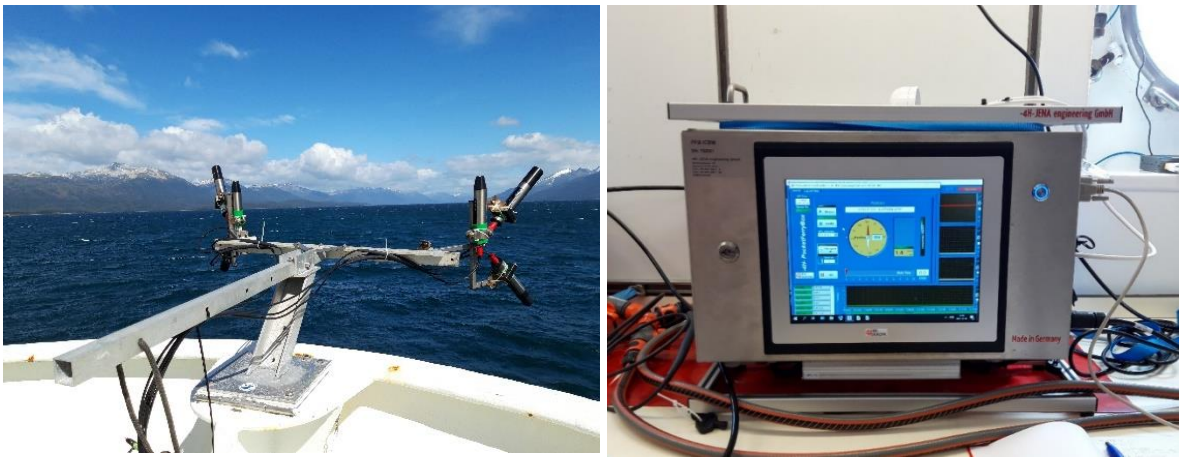

Fig. 5.4.1: Left: Radiometric setup, Right: FerryBox-System

The onboard analyses included measurements of the absorption coefficients of the water sample. They were performed on the unfiltered water as well as on aliquots filtered for the dissolved fraction (0.2 µm). The measurements were done using a point-source integrating cavity absorption meter (PSICAM) and will be set in context with the variables derived from the radiometric observations after the cruise. Furthermore, dissolved organic matter (DOM, material <0.2 µm) was investigated by Excitation-Emission-Matrix (EEM) spectroscopy. In combination with parallel factor analysis (PARAFAC), the data will be used to differentiate fractions within the DOM pool. This allows conclusions about the origin of the DOM (e.g., marine vs. terrigenous) and transformation processes (e.g., bacterial and photochemical degradation). From samples taken underway, aliquots will be stored for analysis in the home laboratory after the cruise. This includes samples for taxonomic composition of phytoplankton for later analysis using a FlowCam instrument.

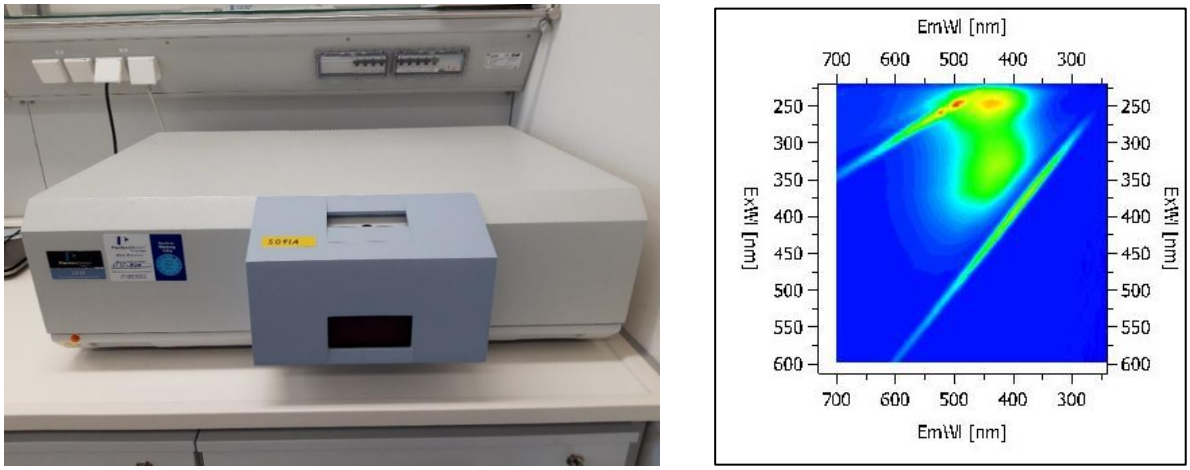

Fig. 5.4.2: Hyperspectral Fluorometer and resulting Excitation-Emission-Matrix (EEM)

5.4.3 Preliminary Results

The figures below give some examples for data obtained by the FerryBox system. In general, the conditions were relatively constant during the transit, what was expected for these oligotrophic waters. However, salinity, turbidity and chl-a fluorescence showed a slight increase from the start to the end of the transit. The data gap around the 25.08.2023 occurred due to the passage through the EEZ of the Cocos-Islands. The steep decline after initially high values that is visible in the oxygen data after the data gap and to the start of the transit is probably an artifact coming from the ships seawater-system. It had to be deactivated in the EEZ of Indonesia and the Cocos-Islands, respectively, and after activation there was a lot of air bubbles in the system, which then also passed the FerryBox and caused these unusual high values. To a certain degree, also the turbidity sensor was affected (high and noisy values on the 24.08.2023). The daily increase/decrease of the chl-a fluorescence values reflects most likely not an actaul variation in phytoplankton biomass, but rather its light acclimatization, thus the non-photochemical quenching of fluorescence. However, this will be further analyzed by a comparison of these data with the discrete absorption coefficients data.

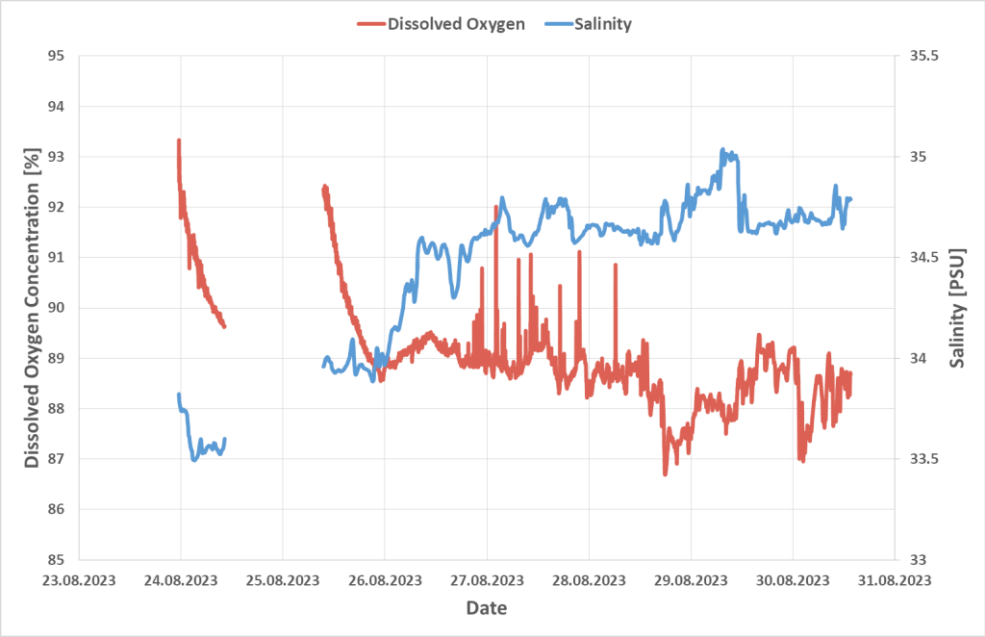

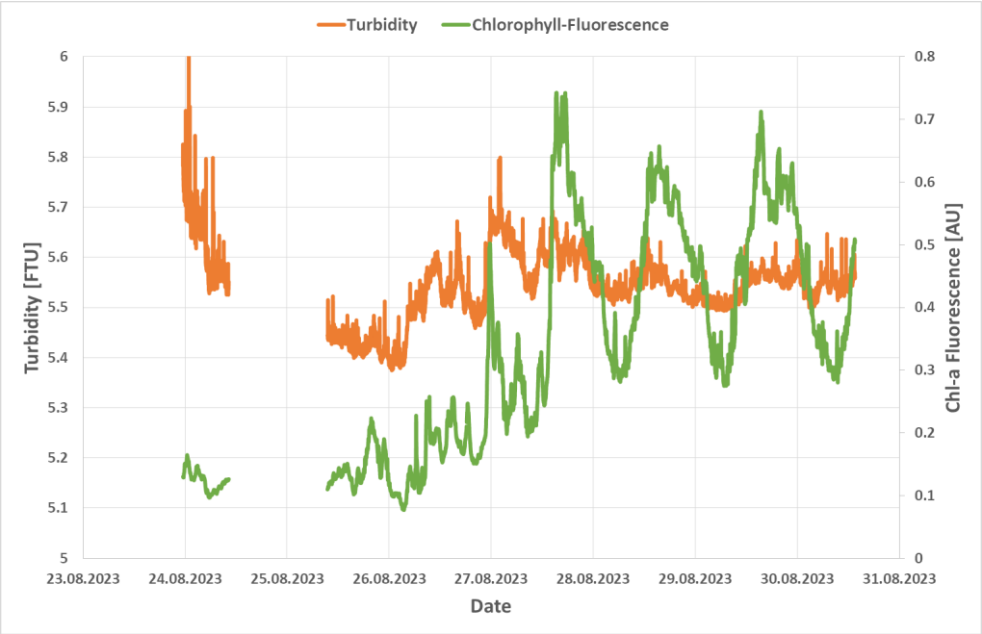

Fig. 5.4.3: Progression of rawdata for dissolved oxygen, salinity, turbidity and chl-a fluorescence during the transit as measured by the FerryBox

5.4.4 Expected Results

From the radiometer setups mounted on the ship's bow, continuous readings of remote sensing reflectance (Rrs; relation of water leaving radiance to downwelling irradiance) will be calculated. They will serve as reference for satellite observations in this area and as the basis to calculate ocean color products (e.g., chl-a concentration). As the radiometers collect light from the first optical depth, these data will probably be not always identical with the measurements obtained in the surface water made by the FerryBox. A comparison of both data sets will thus provide information about vertical chl-a distribution.

The bio-optical measurements performed in the laboratory on discrete samples are expected to give not only on the concentration of dissolved organic matter in the surface water (thus serving as reference for the continuous FerryBox measurements), but also the position and intensity of fluorescence peaks due to the hyperspectral excitation-emission-matrix (EEM) method. This data can be used to further characterize the composition of the dissolved organic matter the ship crossed during the cruise. Lab references will also be used to validate the onboard SMBs in the context of the DAM validation of optical sensors and will therefore support the quality control procedures. The absorption coefficient measurements will further be evaluated for absorption-based phytoplankton biomass proxies, which will be compared with the chl-a fluorescence values of the FerryBox and the chl-a values derived from the radiometric measurements.

5.5 Underway Research Data

(M. Urlaub[1], M. Schlundt[1], R. Kopte[2])

[1]GEOMAR, [2]Kiel University

During the transit track of RV SONNE cruise SO299/2 from Indonesia to Mauritius several data sets were acquired in international waters as part of the German Marine Research Alliance's underway research data project (DAM Underway). Data were recorded on 24/08/2023 between the EEZs of Indonesia and Australia and from 24/08/2023 – 31/08/2023 between the EEZs of Australia and Mauritius. DAM Underway will make this data available to the general public.

5.5.1 Shipboard ADCP current measurements (38 kHz and 75kHz)

Current velocities of the upper water column along the transit track of RV Sonne cruise SO299/2 from Indonesia to Mauritius were collected by two vessel-mounted RDI Ocean Surveyor ADCPs (38 kHz and 75 kHz). The ADCP transducers were located at 6.0 m below the water line. The 38 kHz ADCP was operated in narrowband mode (WM10) with a bin size of 32 m, a blanking distance of 16 m, and a total of 50 bins, the 75 kHz ADCP was operated in narrowband mode (WM10) with a bin size of 8 m, a blanking distance of 8 m, and a total of 100 bins.

Beam velocities as recorded by the data acquisition software VmDAS were transformed to ship coordinates and after merging with the navigation data from the ship's Motion Reference Unit and Global Positioning systems into earth coordinates.

Accuracy of the ADCP velocities mainly depends on the quality of the position fixes and the ship's heading data. Further errors stem from a misalignment of the transducer with the ship's centerline. All acquired raw data were processed using standardized watertrack calibration routines (Fig. 5.5.1).

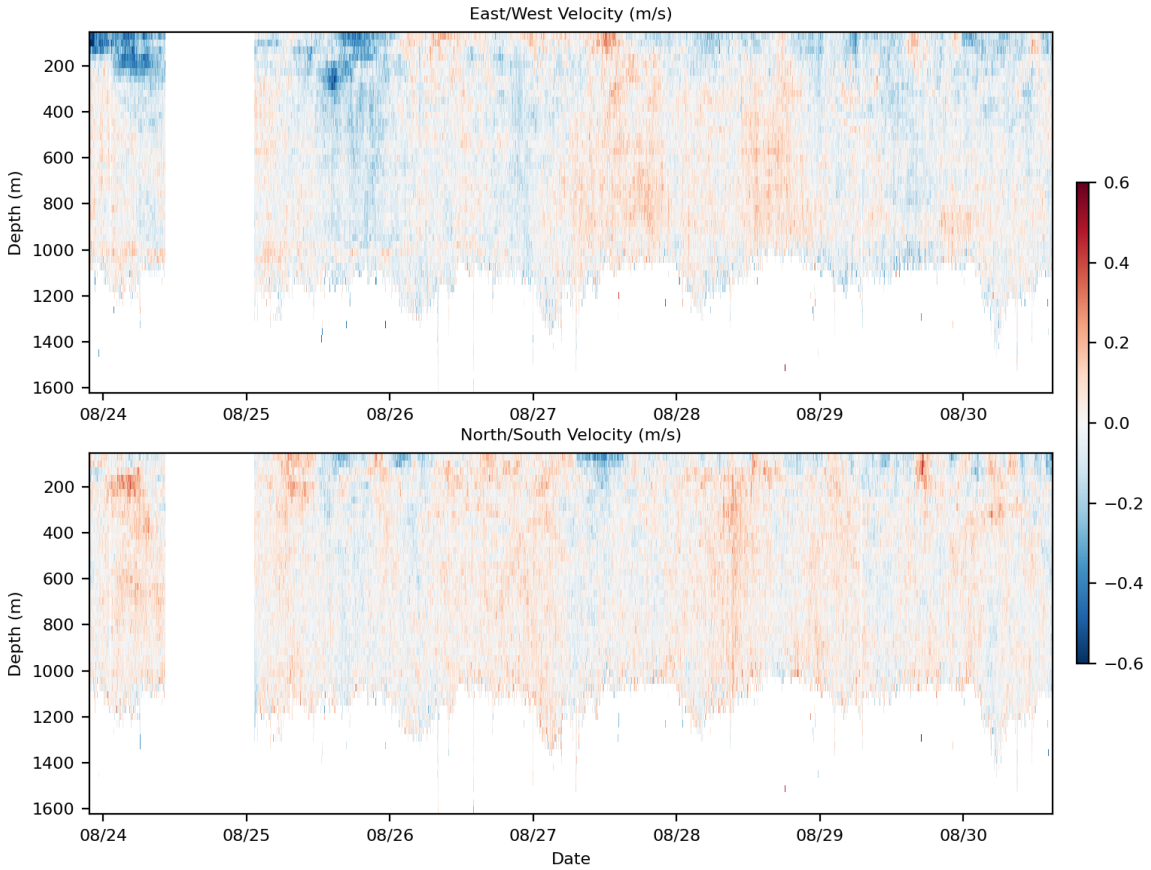

Fig. 5.5.1 Current velocities in the Indian Ocean along the track of SO299/2 derived from 38 kHz ADCP measurements (misalignment angle is -0.0835° and amplitude factor is 1.0005).

5.5.2 Multibeam bathymetry

Swath sonar bathymetry data were recorded in the Indian Ocean using Kongsberg EM122 multibeam echosounder. The approximate average depth is around 5000 m and the opening angle was set to 65°. Sound velocity correction was applied during acquisition using sound velocity profiles measured along the transit (see section 5.1). No manual editing has been applied.

5.5.3 Water sampling

Salinity samples were taken from the seawater system inlet in about 4 m depth. These samples will be measured after the cruise with a salinometer to calibrate the thermosalinograph. The thermosalinograph (TSG) measured the temperature and the salinity throughout the whole cruise whenever it was permitted. Temperature is measured directly at the seawater inlet with a seabird SBE38 thermometer. Salinity is obtained from measurements of internal temperature and conductivity, both measured with a Seabird SBE45. The SBE45 is part of the SMB. Salinity samples were taken along the cruise track from a faucet close to the seawater system inlet in about 4m depth. These samples will be measured afterwards back in the lab with a salinometer to calibrate the TSG salinity.

5.6 Argo Float deployment

(M. Urlaub[1], Daniela Voss[2], G. Semolini Pilo[3])

[1]GEOMAR, [2]ICBM, [3]CSIRO

On behalf of the Australian Argo Float program five free drifting profiling floats were deployed en route at 87°E, 84°E, 81°E, 75°E and 65°E (Fig. 5.6.1). These floats drift with the ocean currents and move up and down between the surface and a mid-water level. The floats' trajectories and other information can be found at: https://fleetmonitoring.euro-argo.eu/dashboard?Status=Active.

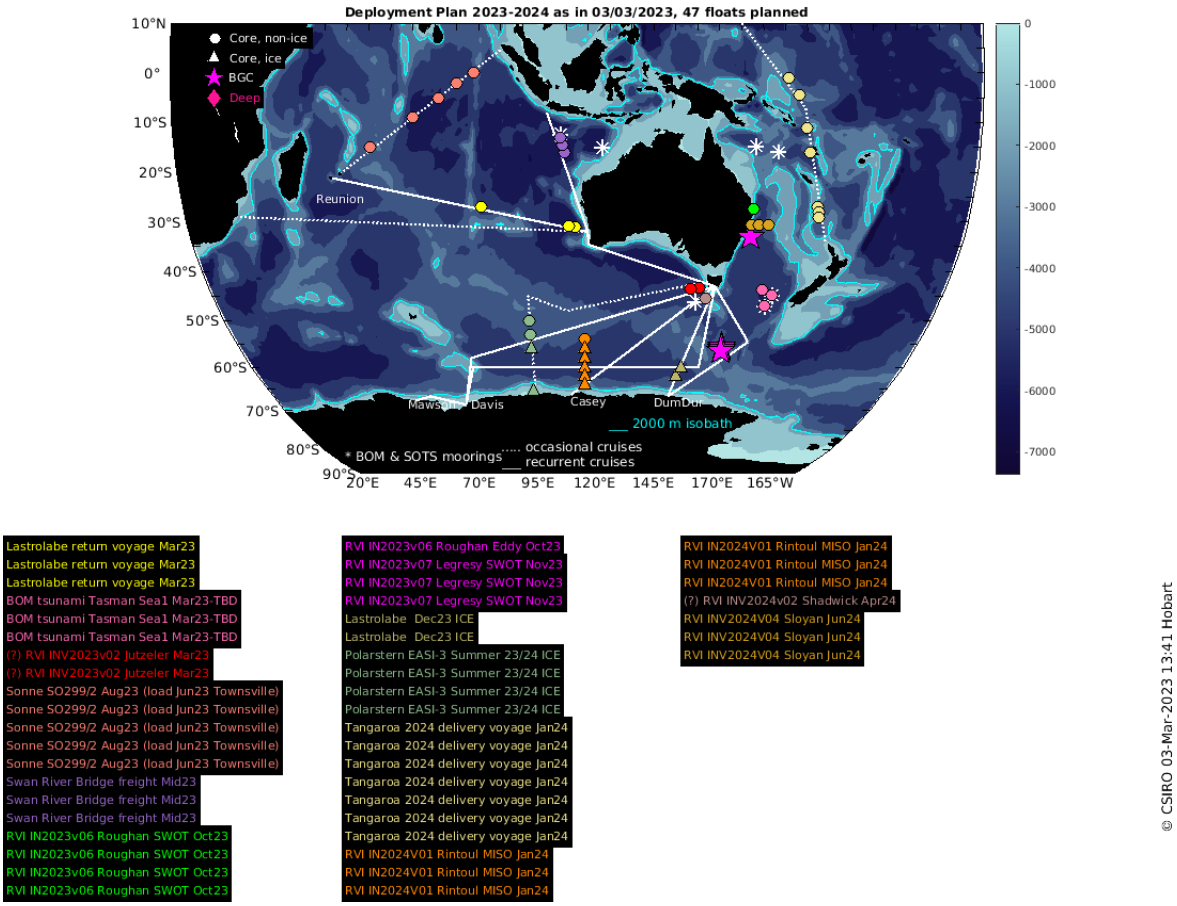

Fig 5.6.1: Deployment plan of the Australian Argo float program including floats that were deployed during SO299/2 (salmon-coloured dots).

7 Station List SO299/2

7.1 Overall Station List

Station No.		Date and Time	Gear	Latitude	Longitude	Water Depth	Remarks/Recovery
Sonne		[UTC]		[°S]	[°E]	[m]	
0	SO299/2_0_Underway-1	19.08.2023 04:35	WISS-DATA	05° 55.321' S	105° 43.669' E	3.5	Parasound, EM710
0	SO299/2_0_Underway-1	21.08.2023 22:45	WISS-DATA	05° 54.286' S	105° 44.336' E	60.9	Parasound, EM710
1	SO299/2_1-1	19.08.2023 06:29	XSV	06° 08.135' S	105° 33.426' E	65.7	XSV01 XSV01.asvp
2	SO299/2_2-1	19.08.2023 07:02	SEISSRC	06° 09.664' S	105° 37.015' E	57.1	Start P1000 (Part 1)
2	SO299/2_2-1	20.08.2023 09:15	SEISSRC	06° 09.254' S	105° 12.443' E	669.1	End P1000 (Part 1)
3	SO299/2_3-1	20.08.2023 07:02	XSV	06° 08.992' S	105° 21.333' E	90.4	XSV02 XSV02.asvp
4	SO299/2_4-1	20.08.2023 12:18	GC	06° 08.989' S	105° 00.865' E	379.5	GC1 (no recovery)
4	SO299/2_4-2	20.08.2023 13:33	GC	06° 08.984' S	105° 00.928' E	383.9	GC2 (no recovery)
5	SO299/2_5-1	20.08.2023 15:00	GC	06° 04.784' S	104° 59.807' E	943.4	GC3 KIEL0257GCK5401
5	SO299/2_5-2	20.08.2023 15:48	GC	06° 04.699' S	104° 59.880' E	848.9	GC4 KIEL0257GCL5401
6	SO299/2_6-1	20.08.2023 19:11	GC	06° 05.377' S	105° 17.992' E	100.5	GC5 KIEL0257GCM5401
7	SO299/2_7-1	20.08.2023 20:00	GC	06° 07.257' S	105° 19.995' E	83	GC6 KIEL0257GCN5401
8	SO299/2_8-1	20.08.2023 22:13	GC	06° 07.768' S	105° 31.352' E	49.6	GC7 KIEL0257GCO5401
8	SO299/2_8-2	20.08.2023 22:39	GC	06° 07.770' S	105° 31.355' E	49.8	GC8 KIEL0257GCP5401
9	SO299/2_9-1	20.08.2023 23:42	GC	06° 07.853' S	105° 31.692' E	56.8	GC9 KIEL0257GCQ5401
10	SO299/2_10-1	21.08.2023 00:39	SEISSRC	06° 07.849' S	105° 31.693' E	57.1	Start P1000 (Part 2)
10	SO299/2_10-1	21.08.2023 18:11	SEISSRC	06° 08.581' S	105° 10.008' E	837.9	End P1000 (Part 2)
11	SO299/2_11-1	21.08.2023 06:59	XSV	06° 12.845' S	105° 21.722' E	102.2	XSV03 XSV03.asvp
0	SO299/2_0_Underway-3	23.08.2023 21:10	ADCP	07° 46.200' S	100° 04.865' E	5546.6	Switch on
0	SO299/2_0_Underway-3	24.08.2023 10:20	ADCP	08° 31.149' S	097° 29.082' E	5442.9	Switch off (EEZ)
0	SO299/2_0_Underway-3	25.08.2023 01:37	ADCP	09° 31.069' S	094° 00.896' E	5305.5	Switch on
0	SO299/2_0_Underway-3	30.08.2023 15:00	ADCP	17° 02.421' S	067° 27.952' E		Switch off (EEZ)
0	SO299/2_0_Underway-5	23.08.2023 21:10	EM122	07° 46.222' S	100° 04.790' E	5536	Switch on
0	SO299/2_0_Underway-5	24.08.2023 10:20	EM122	08° 31.121' S	097° 29.182' E	5451.5	Switch off (EEZ)
0	SO299/2_0_Underway-5	25.08.2023 01:16	EM122	09° 30.170' S	094° 04.073' E	5308.5	Switch on
0	SO299/2_0_Underway-5	30.08.2023 15:00	EM122	17° 02.421' S	067° 27.952' E		Switch off (EEZ)
0	SO299/2_0_Underway-2	23.08.2023 21:10	UWS	07° 46.225' S	100° 04.781' E	5533.9	Switch on
0	SO299/2_0_Underway-2	24.08.2023 10:20	UWS	08° 31.104' S	097° 29.240' E	5451.5	Switch off (EEZ)

0	SO299/2_0_Underway-2	25.08.2023 01:37	UWS	09° 31.061' S	094° 00.920' E	5309.8	Switch on
0	SO299/2_0_Underway-2	30.08.2023 15:00	UWS	17° 02.421' S	067° 27.952' E		Switch off
12	SO299/2_12-1	26.08.2023 08:00	XSV	11° 12.299' S	088° 07.898' E	4471.2	XSV04
13	SO299/2_13-1	26.08.2023 14:04	FLOAT	11° 31.175' S	087° 01.979' E	4953	WMO ID 5905547
14	SO299/2_14-1	27.08.2023 07:11	FLOAT	12° 22.901' S	084° 00.452' E	5374.1	WMO ID 5905548
15	SO299/2_15-1	28.08.2023 01:00	FLOAT	13° 24.888' S	080° 21.847' E	4672.5	WMO ID 5905549
16	SO299/2_16-1	28.08.2023 09:00	XSV	13° 53.487' S	078° 41.016' E	4917.5	XSV05 (no data)
17	SO299/2_17-1	29.08.2023 02:28	FLOAT	14° 55.896' S	075° 00.036' E	5235.5	WMO ID 1901766
18	SO299/2_18-1	30.08.2023 08:59	XSV	16° 43.623' S	068° 35.463' E	3308.2	XSV06
19	SO299/2_19-1	30.08.2023 11:31	FLOAT	16° 51.366' S	068° 07.689' E	3026.3	WMO ID 1901767

7.2 Profile Station List

Line No.	Date Start	Time Start	Date End	Time End	Lon Start	Lat Start	Lon End	LatEnd	FFN Start	FFN End
GEOMAR	2023	[UTC]	2023	[UTC]	[°]	[°]	[°]	[°]		
1001	19.08.	07:26:50.150	19.08.	09:00:10.150	105.5953	-6.1543	105.4740	-6.1268	200	1320
1002	19.08.	09:00:15.150	19.08.	09:26:00.150	105.4740	-6.1267	105.4866	-6.1039	1321	1630
1003	19.08.	09:26:05.150	19.08.	12:53:30.150	105.4867	-6.1039	105.4461	-6.3708	1631	4120
1004	19.08.	12:53:35.150	19.08.	18:03:05.150	105.4462	-6.3708	105.5929	-6.1900	4121	7835
1005	19.08.	18:03:10.150	19.08.	20:14:20.150	105.5929	-6.1900	105.4172	-6.2023	7836	9410
1006	19.08.	20:14:25.150	19.08.	23:22:20.150	105.4171	-6.2022	105.2480	-6.0383	9411	11665
1007	19.08.	23:22:25.150	20.08.	00:51:05.150	105.2481	-6.0383	105.3392	-6.0012	11666	12730
1008	20.08.	00:51:10.150	20.08.	04:29:25.150	105.3393	-6.0013	105.3041	-6.2692	12731	15350
1009	20.08.	04:29:30.150	20.08.	06:46:55.150	105.3041	-6.2692	105.3766	-6.1504	15351	17000
1010	20.08.	06:47:00.150	20.08.	08:57:25.150	105.3765	-6.1504	105.2199	-6.1533	17001	18566
1011	21.08.	00:51:30.150	21.08.	03:02:25.150	105.5308	-6.1280	105.6064	-6.0474	18629	20200
1012	21.08.	03:02:30.150	21.08.	03:09:30.150	105.6064	-6.0474	105.6121	-6.0519	20201	20285
1013	21.08.	03:09:35.150	21.08.	06:04:55.150	105.6121	-6.0520	105.4147	-6.2510	20286	22390
1014	21.08.	06:05:00.150	21.08.	08:21:35.150	105.4146	-6.2510	105.2865	-6.1604	22391	24030
1015	21.08.	08:21:40.150	21.08.	12:00:45.150	105.2865	-6.1604	105.2759	-5.9079	24031	26660
1016	21.08.	12:00:50.150	21.08.	13:15:20.150	105.2760	-5.9079	105.3475	-5.9024	26661	27555
1017	21.08.	13:15:25.150	21.08.	16:16:10.150	105.3476	-5.9025	105.3050	-6.1299	27556	29725
1018	21.08.	16:16:15.150	21.08.	17:53:55.150	105.3049	-6.1299	105.1825	-6.1412	29726	30898

7.3 Sample Station List

Station No.	Date and Time	Gear	Latitude	Longitude	Water Depth	Remarks
Sonne	[UTC]		[°S]	[°E]	[m]	e.g. IGSN number
SO299/2_5-1	20.08.2023 15:00	GC	06° 04.784' S	104° 59.807' E	943.4	KIEL0257GCK5401
SO299/2_5-2	20.08.2023 15:48	GC	06° 04.699' S	104° 59.880' E	848.9	KIEL0257GCL5401
SO299/2_6-1	20.08.2023 19:11	GC	06° 05.377' S	105° 17.992' E	100.5	KIEL0257GCM5401

SO299/2_7-1	20.08.2023 20:00	GC	06° 07.257' S	105° 19.995' E	83	KIEL0257GCN5401
SO299/2_8-1	20.08.2023 22:13	GC	06° 07.768' S	105° 31.352' E	49.6	KIEL0257GCO5401
SO299/2_8-2	20.08.2023 22:39	GC	06° 07.770' S	105° 31.355' E	49.8	KIEL0257GCP5401
SO299/2_9-1	20.08.2023 23:42	GC	06° 07.853' S	105° 31.692' E	56.8	KIEL0257GCQ5401
SO299/2_5-1	20.08.2023 15:00	GC	06° 04.784' S	104° 59.807' E	943.4	KIEL0257GCK5401
SO299/2_5-2	20.08.2023 15:48	GC	06° 04.699' S	104° 59.880' E	848.9	KIEL0257GCL5401
SO299/2_6-1	20.08.2023 19:11	GC	06° 05.377' S	105° 17.992' E	100.5	KIEL0257GCM5401

The sample list for porewater, sediment geochemistry, and tephra is given in Table 5.3.1.

8 Data and Sample Storage and Availability

The metadata of the onboard DSHIP-System is collected and made publicly available by the Kiel Data Management Team (KDMT) through its information and data archival system Ocean Science Information System (OSIS-Kiel). The system is accessible for all project participants and can be used to share and edit field information and to provide scientific data, as they become available. OSIS provides information on expeditions and the availability of data files from completed cruises. The visibility of the research activities and available data is meant to foster collaboration with external scientists. The KDMT will act as data curator and publish the data in the World Data Center PANGAEA. This will ascertain long-term archival and access to the data. The data publication process will be based on the available files in OSIS and is therefore transparent to all reviewers and scientists. This cooperation with a world data center will make the data globally searchable, and links to the data owners will provide points of contact to project-external scientists.

Multibeam field data will be stored at the bathymetric data repository of the Bundesamt für Seeschiffahrt und Hydrografie (BSH) after the cruise. Data collected during transit from Indonesia to Mauritius outside the respective EEZ zones will be archived and made publicly accessible as part of the pilot project DAM (Deutsche Alliance Meeresforschung) Underway Research Data (DAM URD). The ICBM Oldenburg collected underwater samples for marine optics and ocean color remote sensing (Bio-optics) during the transit as part of the second phase of the DAM URD project. The seismic, bathymetric and hydro-acoustic raw data as well as processed seismic data will be archived on a dedicated server at GEOMAR. However, seismic raw data has been included in the DAM URD archiving procedure which will be transferred to PANGEA, and seismic track lines will be visualized on marine-data.de. The data acquired by the Argo Floats is available in near-real time when the float reaches the surface and transmits data before the next dive, which corresponds to every ~10 days. The data sets will be available after the assigned moratorium as listed in Table 8.1.

Table 8.1 Overview of data availability

Type	Database	Availability	Free Access	Contact
Ship's Metadata	BSH, OSIS (Kiel)	October 2023	October 2023	
PARASOUND	GEOMAR	October 2023	October 2027	murlaub@geomar.de
Multibeam	BSH, PANGAEA	October 2023	October 2027	murlaub@geomar.de
SV Profiles	GEOMAR	October 2023	October 2027	murlaub@geomar.de
2D MCS	GEOMAR, PANGAEA	October 2023	October 2027	murlaub@geomar.de
Cores	GEOMAR	October 2023	October 2023	murlaub@geomar.de
Bio-Optics	PANGAEA	October 2023	October 2025	Jochen.wollschlaeger@uol.de
DAM URD	PANGAEA	October 2023	October 2025	www.pangaea.de
Argo Floats	Argo GDACs (Global Data Acquisition Centres)	near-real time, from the time of deployment	near-real time, from the time of deployment	https://argo.ucsd.edu/data/data-from-gdacs/ Gabriela.Semolinipilo@csiro.au

9 Acknowledgements

We are grateful to the Government of the Republic of Indonesia for granting permission to work in Indonesia's Exclusive Economic Zone. Our special thanks go to BRIN, especially Dr.-Ing. Semeidi Husrin (Head of Coastal Engineering & Disaster Mitigation) and the German Embassy in Jakarta, especially Annisa Fitria (Head of Science & Technology Division), for obtaining research and other permits and for their help around the RV SONNE port activities.

We appreciate the effective assistance of the team at the Leitstelle, especially their help and persistence during the preparatory phase. The great support of Captain Meyer and his crew helped tremendously to make the cruise a success – thank you!

Cruise SO299/2 was realized thanks to funding from BMBF (03G0299TA) and GEOMAR. This project has further received funding from the European Research Council (ERC) under the European Union's Horizon 2020 research and innovation program (grant agreement No. 948797).

10 References

Abdurrachman, M., Widiyantoro, S., Priadi, B. and Ismail, T., 2018. Geochemistry and structure of krakatoa volcano in the Sunda Strait, Indonesia. *Geosciences*, 8(4), p.111.

Cutler, K.S., Watt, S.F., Cassidy, M., Madden-Nadeau, A.L., Engwell, S.L., Abdurrachman, M., Nurshal, M.E., Tappin, D.R., Carey, S.N., Novellino, A. and Hayer, C., 2022. Downward-propagating eruption following vent unloading implies no direct magmatic trigger for the 2018 lateral collapse of Anak Krakatau. *Earth and Planetary Science Letters*, 578, p.117332.

Gardner, M.F., Troll, V.R., Gamble, J.A., Gertisser, R., Hart, G.L., Ellam, R.M., Harris, C. and Wolff, J.A., 2012. Crustal differentiation processes at Krakatau volcano, Indonesia. *Journal of Petrology*, 54(1), pp.149-182.

Neumann van Padang, M., 1933. De Krakatau voorheen en thans. *De Tropische Natuur*, 22(8), pp.137-150.

PVMBG, 2022. Accessed 28/08/2023, <https://vsi.esdm.go.id/index.php/gunungapi/aktivitas-gunungapi/3973-peningkatan-tingkat-aktivitas-g-anak-krakatau>

Sargent, J.R., 1976. The structure, metabolism and function of lipids in marine organisms. In: Malins, D.C., Sargent, J.R. (Eds.), Biochemical and Biophysical Perspectives in Marine Biology. Academic Press, London, pp. 149-212.

Self, S., 1992. Krakatau revisited: the course of events and interpretation of the 1883 eruption. *GeoJournal*, 28, pp.109-121.

Smith, K.L., Ruhl, H.A., Kaufmann, R.S., Kahru, M., 2008. Tracing abyssal food supply back to upper-ocean processes over a 17-year time series in the northeast Pacific. Limnology and Oceanography 53, 2655-2667.

Sudradjat, A., 1983. The Morphological development of Krakatau volcano. *In Proceedings of the workshop on coastal resources management of Krakatau and the Sunda Strait Region, Indonesia, 1983 (*pp. 22-31).

Susilohadi, S., Gaedicke, C., & Djajadihardja, Y., 2009. Structures and sedimentary deposition in the Sunda Strait, Indonesia. *Tectonophysics*, 467(1-4), 55-71.

Umbgrove, J.H.F., 1928. The first days of the new submarine volcano near Krakatoa. *Leidse Geologische Mededelingen*, 2(1), pp.325-328.

Whittaker, R.J., Bush, M.B. and Richards, K.J.E.M., 1989. Plant recolonization and vegetation succession on the Krakatau Islands, Indonesia. *Ecological Monographs*, 59(2), pp.59-123.

Whittaker, R.J., Walden, J. and Hill, J., 1992. Post-1883 ash fall on Panjang and Sertung and its ecological impact. *GeoJournal*, 28, pp.153-171.

11 Abbreviations

ADCP	Acoustic Doppler Current Profiler
BRIN	Badan Riset dan Inovasi Nasional (Indonesia)
BSH	Bundesamt für Seeschiffahrt und Hydrografie
CSIRO	Commonwealth Scientific and Industrial Research Organisation (Australia)
CTD	Conductivity Temperature Depth
DAM	Deutsche Allianz für Meeresforschung
DOM	Dissolved Organic Matter
EEZ	Exclusive Economic Zone
EEM	Excitation-Emission-Matrix
GC	Gravity Core
ICBM	Institut für Chemie und Biologie des Meeres
KDMT	Kiel Data Mangement Team
OSIS	Ocean Science Information System

SMB	Self-cleaning Monitoring Box
TSG	Thermosalinograph
URD	Underway Research Data